2017

Mechanical Property Characterization of Discontinuous Fiber Reinforced Composites by Computer Modeling

Amrit Bhusal
South Dakota State University

MECHANICAL PROPERTY CHARACTERIZATION OF DISCONTINUOUS FIBER REINFORCED COMPOSITES BY COMPUTER MODELING

BY

AMRIT BHUSAL

A thesis submitted in partial fulfillment of the requirement for

Master of Science

Major in Mechanical Engineering

South Dakota State University

2017

MECHANICAL PROPERTY CHARACTERIZATION OF DISCONTINUOUS FIBER REINFORCED COMPOSITES BY COMPUTER MODELING

AMRIT BHUSAL

This thesis is approved as a creditable and independent investigation by a candidate for the Master of Science in Mechanical Engineering degree and is acceptable for meeting the thesis requirements for this degree. Acceptance of this does not imply that the conclusions reached by the candidates are necessarily the conclusions of the major department.

Zhong Hu, PhD. Date:

Thesis Advisor

Kurt Basset, PhD. Date:

Head, Department of Mechanical Engineering

Dean, Graduate School Date:

ACKNOWLEDGEMENTS

I would like to express special thanks to my advisor Dr. Zhong Hu for his support and guidance from the very beginning of my Master's program. His encouragement, patience and kindness throughout my studies was indescribable. I am grateful to Dr. Deepthi Kolady and Dr. Fereidoon Delfanian for being my research committee member and providing valuable suggestions. I am grateful towards Department of Mechanical Engineering at South Dakota State University for giving me opportunity to enroll in Master of Science in Mechanical engineering program.

My sincere appreciation to Brian Moore and University High Performance computing for letting me use their computation facility.

CONTENTS

ABBREVIATIONS

MPa	Mega Pascal
GPa	Giga Pascal
Mm	Millimeter
ROM	Rule of Mixture
RVE	Representative Volume Element.
FEA	Finite Element Analysis
1D	One Dimensional
3D	Three Dimensional
DiF	Discontinuous Fiber

LIST OF FIGURES

LIST OF TABLES

ABSTRACT

MECHANICAL PROPERTY CHARACTERIZATION OF DISCONTINUOUS FIBER REINFORCED COMPOSITES BY COMPUTER MODELING

AMRIT BHUSAL

2017

The desire to make high strength, lightweight, less corrosive, high fatigue resistance materials in auto industries, aero industries, biomedical industries have given a chance for in-depth study of composite materials. To get the profound knowledge of composites, different experiments are conducted which often take huge resources, cost and time.

Computer modeling and analysis have gained popularity in Finite Element Analysis (FEA) because it can be used to predict the mechanical property of different materials. In this thesis, FEA technique has been used to predict mechanical property of discontinuous fiber reinforced composites (FRC). If we are able to foretell the mechanical property of discontinuous fiber reinforced composites (FRC), it can be used- being easy and less expensive to manufacture than continuous discontinuous fiber reinforced composites (FRC).

The objective of this thesis is to find out the behavior of discontinuous fiber reinforced composites under tensile, compressive and shear test. Different volume percentage of random fibers, matrix was generated, which was subjected to FEA simulation. ANSYS 2015, commercially available Finite Element Analysis software, was used to generate model and as a solver.

During tensile test, the model subjected to 1% elongation in one direction and other two directions were kept fixed. Displacement and force at each node was found, and later used to find Young's Modulus and Poisson's Ratio. For shear test, one plane was fixed while the opposite plane was given a deformation of 1%, displacement and force at each node was noted at different length of a model, which was further used to calculate Shear Modulus. Material property like Young's Modulus, Shear modulus increased as the aspect ratio or volume percentage of fiber was increased however Poisson's ratio was decreased as the fiber aspect ratio or volume percentage was increased.

1. INTRODUCTION

Composite materials are made from two or more constituent material, which are combined to get the behavior of individual in a single material. Lightweight, high strength, durability, high corrosion resistance is some of the properties of composite materials. Carbon fiber reinforced composites are unique and is widely recognized for its g strength to weight ratio, very low coefficient thermal expansion and few other properties like high resistance to chemical, biological changes [22]. Composite materials are in high demand in military, aerospace, automotive manufacturing, bio medical application. Advancement in composite research has made its application in more sector like medical field.

Composites are made of two main categories of constituent materials:

1) Matrix

2) Reinforcement

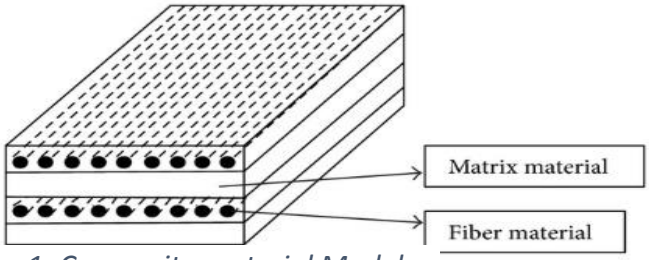

Figure 1: Composite material Model.

Short fiber reinforced composites also known as discontinuous fiber reinforced composites were developed to fill the property gap between continuous fiber laminates and unreinforced polymer. If the fibers in discontinuous fiber reinforced composites are sufficiently long, stiffness of continuous fiber reinforced composites at same fiber loading can be achieved. Difficulty in manufacturing, highly aligned fibers are some of the drawbacks of continuous fiber reinforced composites, which can be overcome by discontinuous fiber reinforced composites, if material properties will be close enough.

Different type of techniques can be used to find the material property of discontinuous fiber reinforced composites. The most reliable is physical testing or experimental method but it comes with high cost, huge resources, and time. Another technique can be computer modeling, where a model is made, and Finite Element Analysis does analysis. We used the computer modeling technique where discontinuous fiber reinforced composite model was made and with the theoretical knowledge of tensile, shear test further analysis was done. ANSYS 2015, commercially available Finite Element Analysis software, was used to generate model and as a solver.

Different approach had been tried to get accurate results from modelling technique. Fu et al calculated the tensile modulus and strength of Discontinuous carbon fiber reinforced thermoplastic in different fiber aspect ratio and orientation based on modified law of mixture [2][3]. An accurate multi scale FE (finite element) model was established by Hashimoto et al to conduct simulation of tensile strength of discontinuous fiber composites with different fiber orientation distribution [5].

1.1 MANUFACTURING PROCESS.

Discontinuous fiber reinforced composites can be manufactured in different ways. Some of them are

- Hand layup
- Resin Infusion Process
- Injection Molding

- Filament Winding
- Automated Fiber Placement
- 3D-Printing

Hand layup is a molding process where fiber reinforcements are placed by hand then wet with resin. The manual nature of this process allows high range of fiber material to be considered. This is one of the oldest method of manufacturing discontinuous fiber reinforced composites.

INJECTION MOLDING

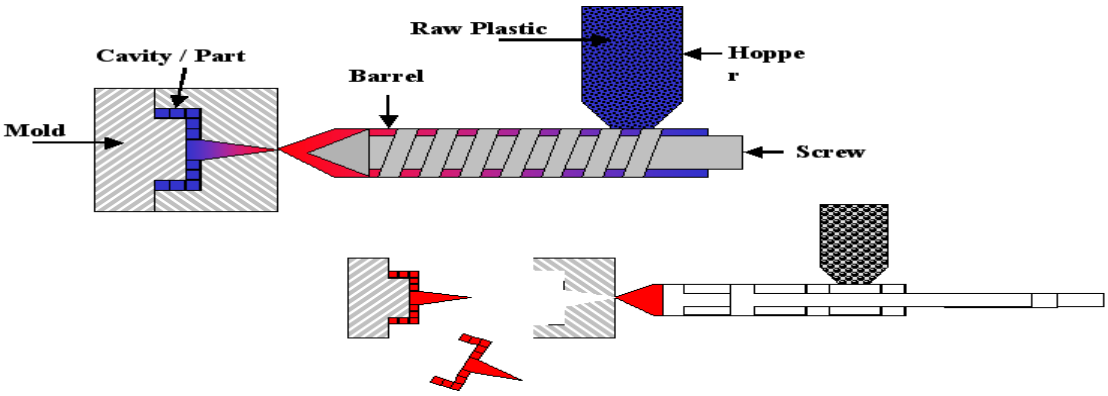

Figure 2: Injection Molding Process. [18]

In, injection molding process two resin components are combined and mixed together, and is feed through feeder towards heated barrel. The resign is injected into a mold, which contains reinforced material. This process is mostly use in automotive industries, military, aero industries. Figure 2 shows the injection molding process.

FILAMENT WINDING

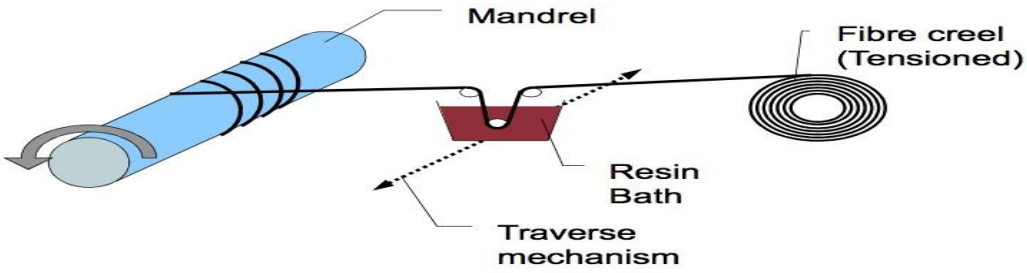

Figure 3: Filament Winding Process. [19]

Filament is either pre-coated with the polymer or is drawn through a polymer bath and is winded in a winder. This process has high productivity rate. Figure 3 shows the filament winding process.

3D PRINTING

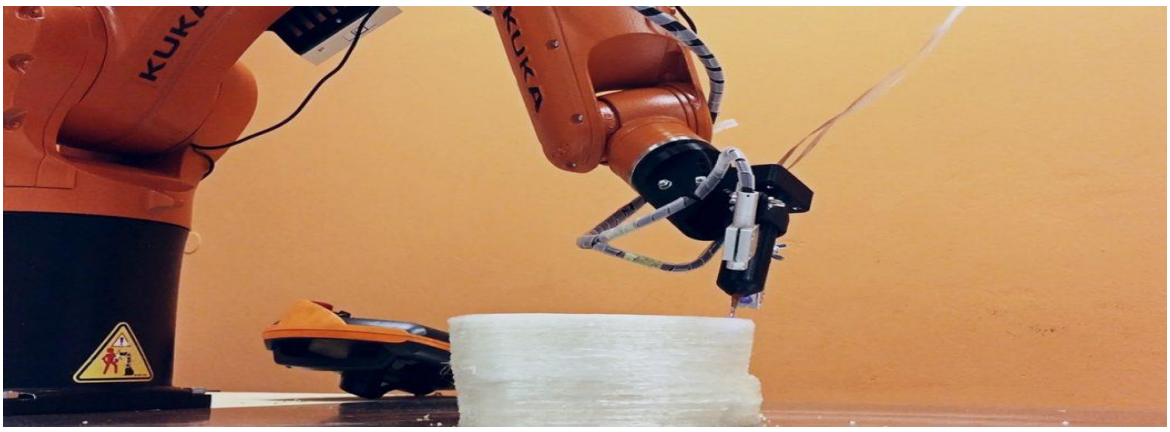

Figure 4: 3D Printing Process. [20]

In this process, three-dimensional object is created, layer by layer, under computer control. This is additive manufacturing process, which is highly used to produce carbon, glass fiber reinforced DiF composites. High precision and wide variety of product are some of its characteristics.

1.2 LITERATURE REVIEW

Looking at the advantages that discontinuous fiber reinforced composites have, researchers invested huge amount of time in looking different behavior of discontinuous fiber reinforced composites. Biometrics has also been a great field for research in order to enhance properties of discontinuous fiber reinforced composites. An effective approach to design cellular periodic composites reinforced by discontinuous fiber reinforced composited is to adopt the ideas behind biomimetic, which can encompass the essential aspects in material design, system engineering, and even business model [23-43]. Different models and theories have been developed to predict the strength and stiffness of discontinuous fiber reinforced composites.

To fulfill the demand of discontinuous fiber reinforced composites in structural, automotive, medical sector, with different material property, knowing the mechanical behavior of discontinuous fiber reinforced composite is most. Change in fiber orientation and fiber volume percentage changes the mechanical property of discontinuous fiber reinforced composites.

Z.HU *et al.* [1] A 13-layer 3D orthogonal fabric composite with binding of warp yarns through the thickness and carbon fiber of 52.65% volume was selected as the case study material. Young's moduli in fiber oriented direction and shear moduli were significantly higher than that of matrix material and the stability of material can be improved with fiber placement.

Material property in discontinuous fiber reinforced composite highly depend on fiber placement and fiber orientation. Material property like Young's Modulus and Shear Modulus are relatively high along the direction of fiber, which, also depends in the aspect ratio, and volume of fiber. Curtis *et al.* [4] the rule of mixture does not directly work for randomly distributed fiber since it does not care about fiber matrix interaction effect and fiber orientation. Different modification of rule of mixture has been done to use it for short fiber reinforced composites.

Experiments and physical testing takes high cost, resources and time so computer modelling can be another technique to extract material property of discontinuous fiber reinforced composite. However, fiber matrix binding and void creation in matrix material can be a problem, which needs to be considered apart from it computational limitation can be an issue when modelling and analyzing. Sedyono *et al.* [6] FEM simulations are generally limited to modelling a Representative Volume Element (RVE) of the material. In fact, the maximum number of elements that is needed to introduce the exact reinforcement geometry in the numerical model is restrained by computational limitations and modelling complexities. [3]

Fiber concentration in discontinuous fiber reinforced composites is one factor, which alters the material property. Different research has shown that more the fiber concentration higher the stiffness of discontinuous fiber reinforced composites. S.Rahmanian et al. [7] the fraction content of carbon nanotubes (CNT) varied from 0.2 to 0.5 wt. percentage of composites combined with

CNT grown short carbon fibers (CSCF). Synergic performance of CNT and CSCF were studied on tensile, thermomechanical and impact properties of multiscale composites. Both tensile strength and modulus of multiscale composites were increased noticeably in comparison to CNT–epoxy or CSCF–epoxy composites.

As we discussed fiber concentration has positive effect on material property, it is also the topic of quest how the orientation of fiber in discontinuous fiber reinforced composites effect the material property. Hiroyuli *ei al* [.8] Fiber orientation is one of the most important factors influencing the mechanical properties of fiber-reinforced composites. The ultimate tensile stress steadily increases with increasing fiber volume fraction.

1.3 MOTIVATION

Appealing mechanical, structural, thermal properties of discontinuous fiber reinforced composites have huge field of applications. Difficulty to manufacture and highly aligned fibers in continuous fiber reinforced composite has given opportunity to study discontinuous fiber reinforced composites.

Real test and experiments for finding mechanical property of a material takes huge money, resources and time so Finite Element Analysis can be used to predict material's stiffness, shear by using computer modelling but discretization of the whole model into Finite Element Model will cost a lot of time and money [44]. Therefore, the homogenization method allows us to evaluate the effective properties of the periodic unit cell [45].

Homogeneous theory, where the simple representative volume of discontinuous fiber reinforced composite is taken and simulated to have the property of entire discontinuous fiber reinforced composites can be used. Young's Moduli, Shear Moduli, Poisson's ratio prediction can give us the knowledge of discontinuous fiber reinforced composites mechanical property, which can be done by making a model of material and further analyzing it.

With the numerous application of discontinuous fiber reinforced composites, a computer modelling technique in prediction of material behavior will be a great step forward in discontinuous fiber reinforced composites manufacturing.

2. METHODOLOGY

Manufacturing continuous fiber composites are difficult and expensive process so we try to get the nearest tensile and shear strength with discontinues fibers. We started with aspect ratio 1,10,20,30,40,60,80 and 100 respectively and again we did some work to know how the composite mechanical property vary with the fiber volume percentage. We were able to get the information up to 18% because of restriction of number of elements in ANSYS student version 14.5. Initially a rectangular matrix was formed, and the random points were generated inside it and at those points, the fibers were generated. For each volume percentage of fiber, the number of fibers also varied. Instead of circular cross section fiber, we used squared cross section for the ease of modelling and meshing. The diameter of the fiber was 7 micrometers, but the length varied with aspect ratio.

The analysis was performed as following flow chart

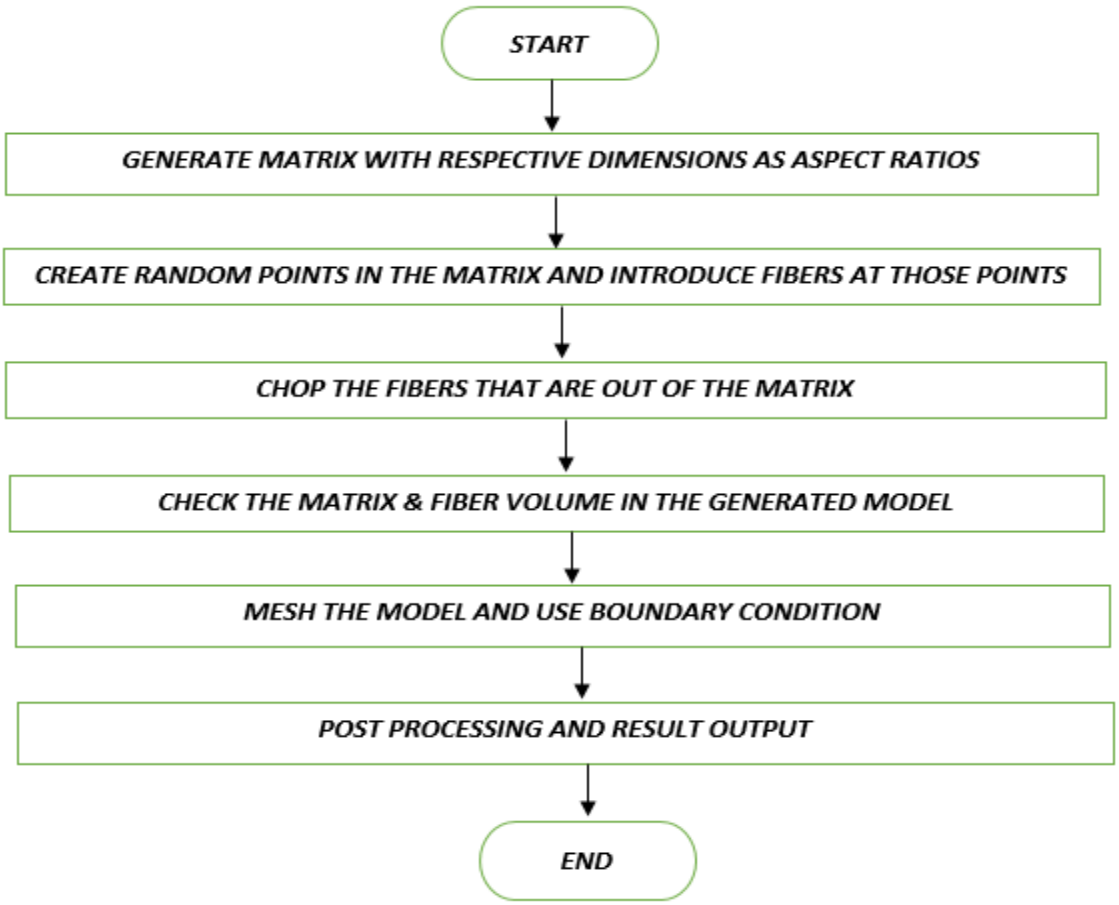

Figure 5: Methodology.

2.1 TEST CONDUCTED

Two different tests were done to find the material property of a discontinuous fiber reinforced composites using computer modelling.

1. Tensile/Compression test
2. Shear test

Tensile Test

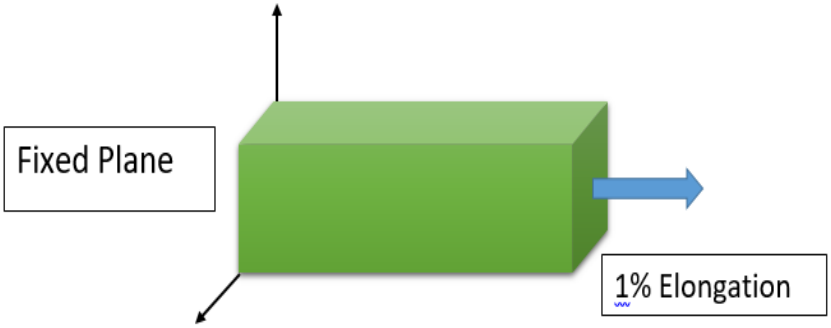

Figure 6: Pictorial representation of tensile test.

Figure 6 shows the pictorial representation of tensile test conducted by computer modeling. The model we created was in cuboid shape as shown in pictorial representation. In order to perform tensile test one edge of the model was kept fixed, which makes displacement along all three directions to be zero i.e. U_x = U_y = U_z = zero. The opposite edge of fixed edge was given elongation of 1% of length, which was the displacement along Z direction i.e. U_z = 1% of length. In our model, Z direction was fiber direction whereas X and Y directions were be fiber transverse directions. The 1% of length elongation of the model acts as the strain, with the given strain we can calculate the force, force and area gives stress which was used for calculating Young's Modulus. Tensile test was conducted in all three directions.

Shear Test

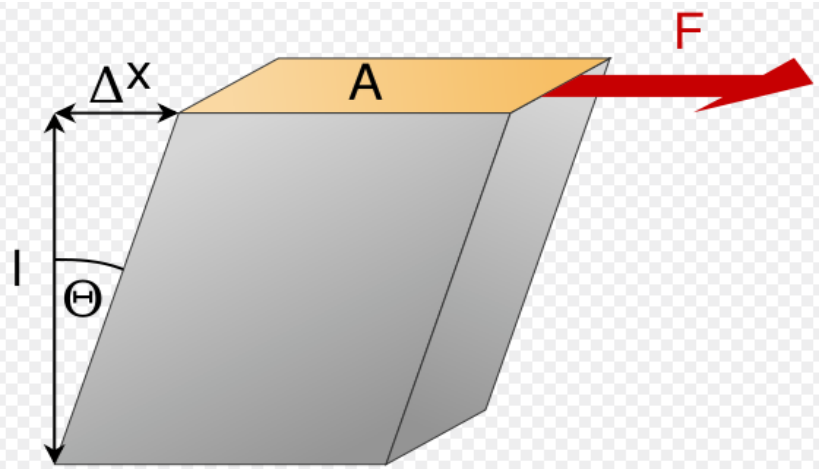

Figure 7: Pictorial representation of Shear. [21]

Figure 7 shows the pictorial representation of shear test done by computer modeling. In order to perform shear test one edge of a model was kept fixed i.e. U_x = U_y = U_z = zero and opposite edge was given deformation of 1% of length i.e. U_z = 1% of length. This given deformation created strain in a model and with that strain, we calculated force and further shear modulus. In order to increase accuracy same process was repeated in three different planes i.e. 0.2-0.4, 0.4-0.6, 0.6-0.8 and the average shear modulus was taken.

2.2 EQUATIONS

Different equations were used in order to calculate Young's modulus shear modulus and Poisson's ratio. Some of the fundamental equations are

YOUNG'S MODULUS.

Young's Modulus is a measure of the stiffness of a material. It is the ratio of stress (force per unit area) to strain (deformation per original length). For our model strain at each node was calculated which was used to calculate Young's Modulus.

$$E=\frac{\text{Stress}}{\text{Strain}}=\frac{\frac{F}{A}}{\frac{dl}{L}}=\frac{F\times L}{dl\times A}$$

Where,

E=Young's Modulus (modulus of elasticity).

F=Force exerted on an object under tension.

A= Cross section area through which force is exerted.

L= Original Length of the object.

dl= Amount by which the length of object changes.

SHEAR MODULUS

Shear Modulus is define as the ratio of shear stress to the shear strain.

$$G=\frac{\text{Shear stress}}{\text{Shear strain}}=\frac{\frac{F}{A}}{\frac{dx}{l}}=\frac{F*l}{dx*A}$$

Where,

G=Shear Modulus (modulus of rigidity).

F=Force exerted on an object under Shear.

A= Cross section area through which force is exerted.

L= Initial length of the object.

dx = transverse displacement.

POSSION'S RATIO

Poisson's ratio is the ratio of transverse strain to axial strain.

$$\nu_{yx} = -\frac{\varepsilon x}{\varepsilon y}$$

Here y direction is the tensile test load direction and x is the strain measurement in the transverse to the tensile load direction.

$$\nu_{xz} = -\frac{\varepsilon z}{\varepsilon x}$$

Here x direction is the tensile test load direction and z is the strain measurement in the transverse to the tensile load direction.

$$\nu_{zx=-}\frac{\varepsilon x}{\varepsilon z}$$

3. MODEL GENERATION

Two step approach was used, where in first step uniaxial (1D) random fibers were generated and the test for tension/compression and shear was done by computer modelling in order to find material properties (Young's Modulus, Shear Modulus and Poisson's ratio). In second step, Monte Carlo method was used where each element of, a composite solid model generated, represented an element of a composite fiber. Tensile/Compression, Shear tests were conducted to find the material property of 3D random discontinuous fibers.

Initially the dimension for the matrix material was set according to aspect ratio and random fibers were generated inside matrix using random coordinates. Fiber radius was fixed as 7 μm but the length was changed as the aspect ratio changed. The analysis was

done with different volume percentage which was 5%,10%,15% and 18%, aspect ratio of fiber used were 1,10,20,30,40,60,80 and 100 .

Table 1 shows the dimensions of matrix block used for different aspect ratios.

BLOCK DIMENSION WITH ASPECT RATIO FOR 1D

Table 1 : Matrix dimensions with different aspect ratio for 1D.

Aspect Ratio(L/d)	Width of block(mm)	Thickness of block(mm)	Length of block(mm)
10	0.1	0.1	0.15
20	0.1	0.1	0.3
30	0.1	0.1	0.45
40	0.1	0.1	0.6
60	0.1	0.1	0.9
80	0.1	0.1	1.15
100	0.1	0.1	1.5

For 3D the block dimension was same for all aspect ratios and it was 40mm*40mm*40mm.

Length of fiber = Aspect ratio × a

In addition, ‘a’ was found using,

$$\pi \times r^2 = a^2$$

Where a, is the width of the fiber and r is seven µm.

Matrix and fiber properties

- Matrix block
    - Young’s Modulus: 2.865e3 MPa.

- Poisson's Ratio: 0.36
- Shear Modulus: 1.053e3 MPa.
- Length vary with aspect ratios.

- Fibers
  - Young’s Modulus along fiber direction: 250e3 MPa.
  - Young’s Modulus along transverse direction:22.4e3 MPa
  - Major Poisson's Ratio:0.35, Minor Poisson's Ratio:0.027

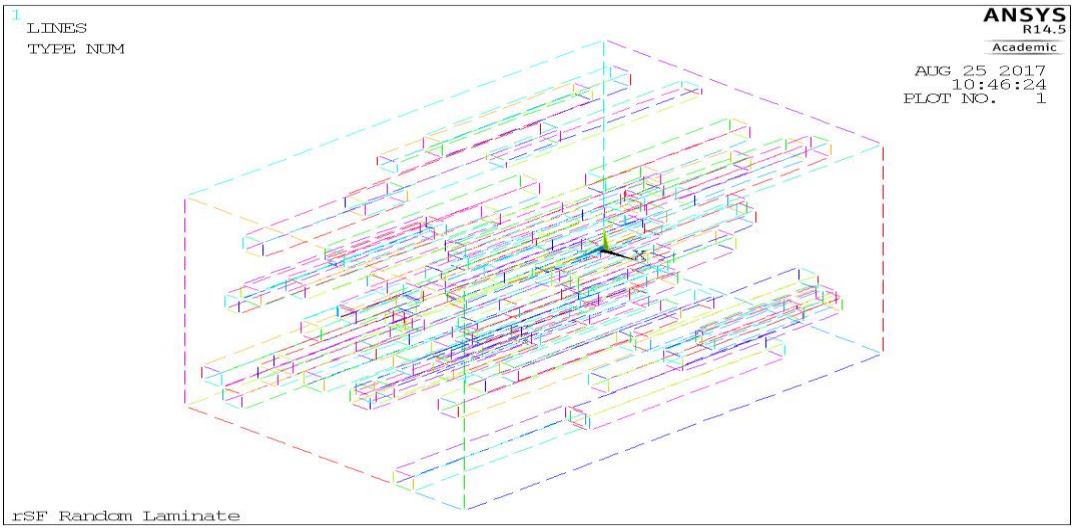

Figure 8: 1D Non- intersecting random fibers for 10 L/D.

Figure 8 shows the line representation of random fiber generated inside matrix for aspect ratio of 10. Fiber inside the matrix are unidirectional and along Z direction.

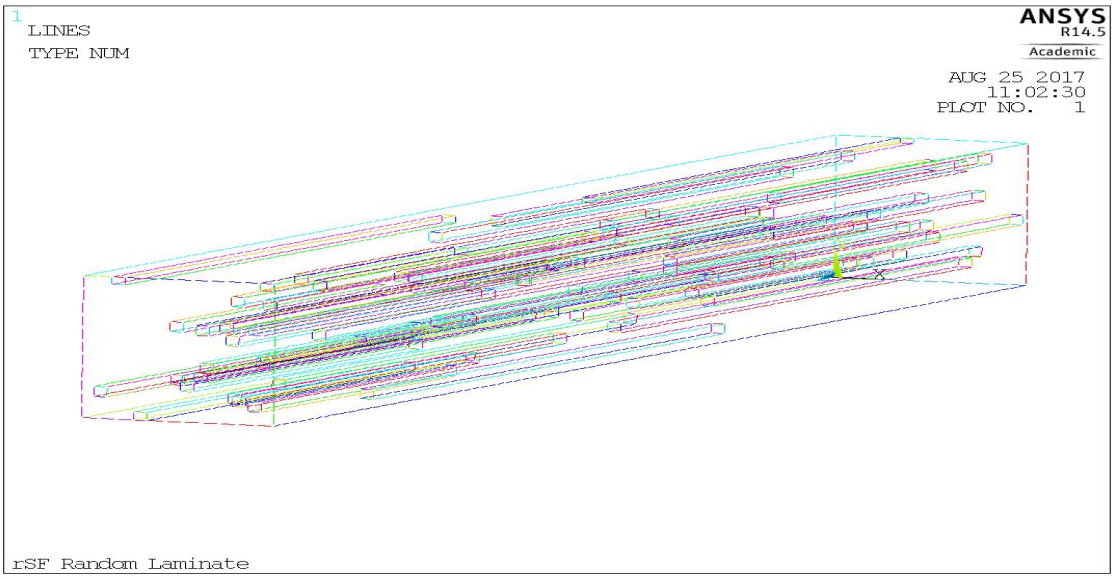

Figure 9: 1D Non-intersecting random fibers for 60 L/D.

Figure 9 shows the line representation of random fiber generated inside the matrix for aspect ratio of 60. Fiber are oriented towards Z direction.

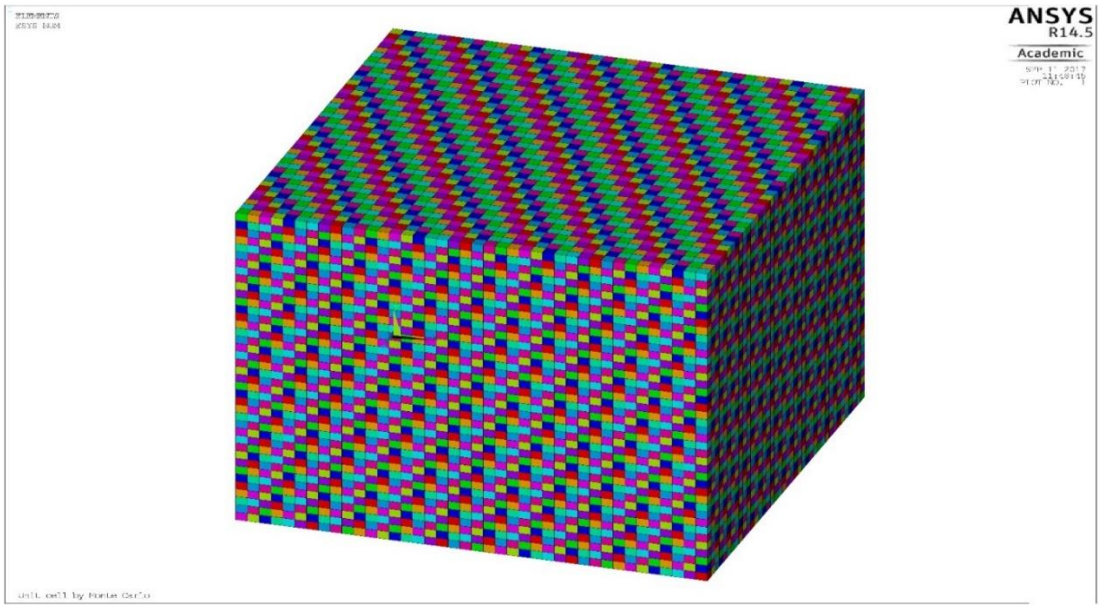

Figure 10: 3D Model.

3.1 DISCRETIZATION AND MESHING.

Fine mesh of fiber and matrix material was desired. The limitation of maximum number of element in ANSYS software was traded with mesh quality. Figure 11 shows the mesh generated in 1D model with aspect ratio of 60.

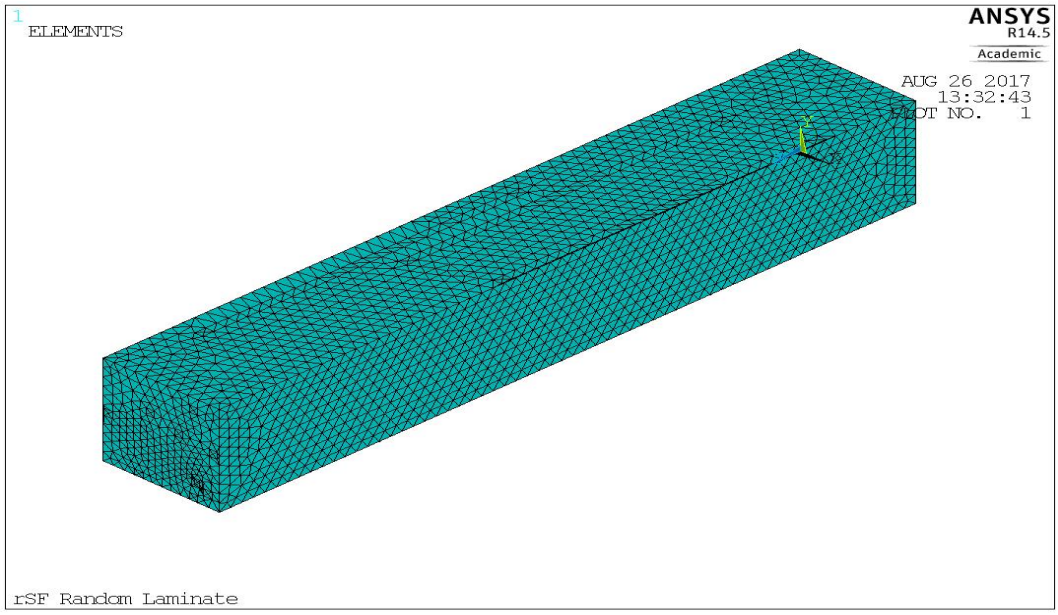

Figure 11: 1D Meshed model with non-intersecting fibers and matrix material.

3.2 BOUNDARY CONDITION AND DIFORMATION

Tensile test and shear test was done for each model where one edge was kept fixed and along the opposite edge 1% length elongation was given. The displacement in all three directions on fixed edge was zero and the displacement on z direction for opposite edge was 1% of length, which was our boundary condition. Figure 12 shows the deformed edge expanded along x direction and is contracted along y direction.

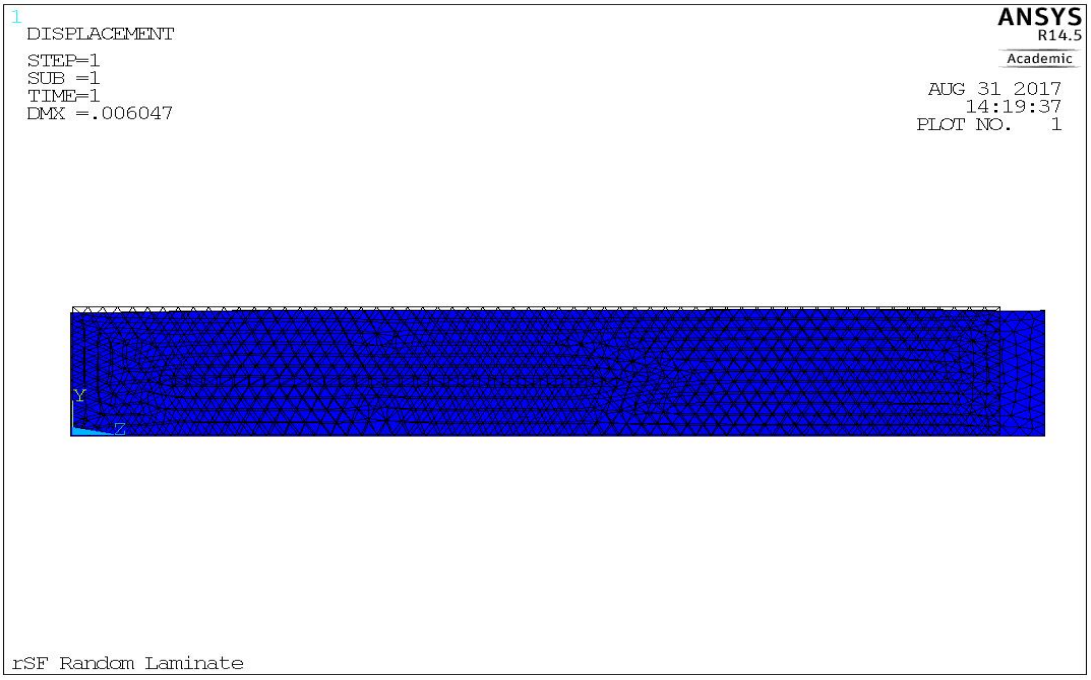

Figure 12: Deformed 1D model for aspect ratio of 40.

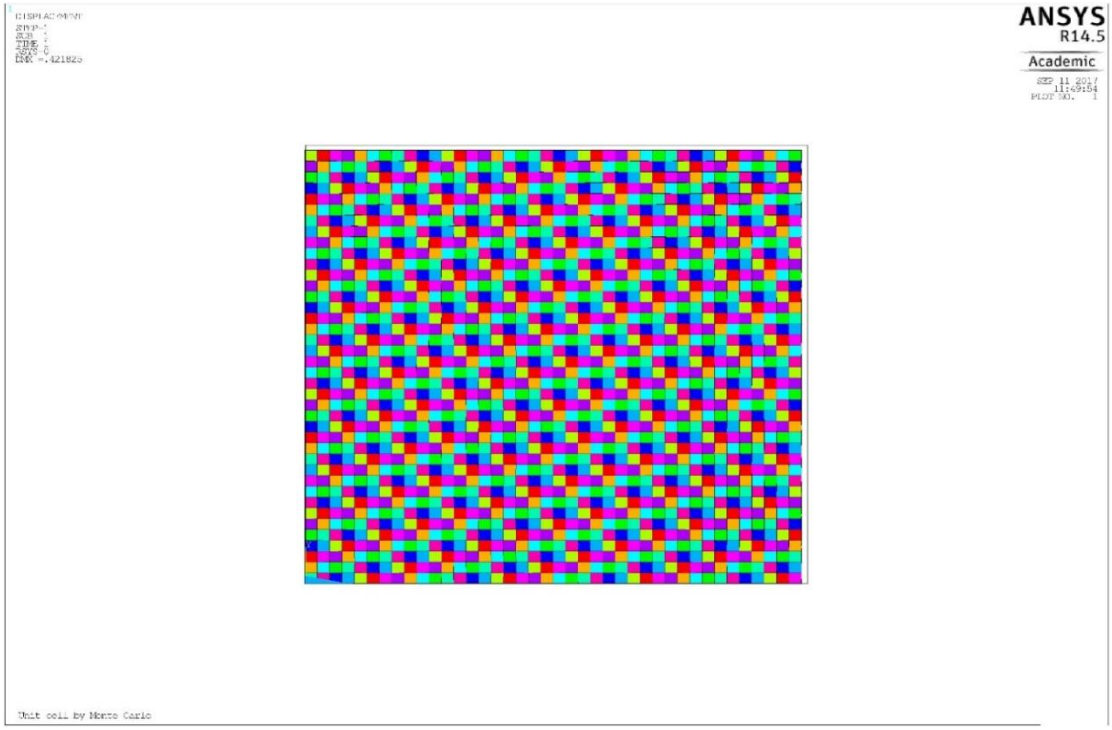

Figure 13: 3D model with deformed edges.

Figure 13 shows the deformed edges and un deformed 3D model of discontinuous fiber reinforced composite.

4. RESULTS AND DISCUSSION

4.1 1D RANDOM FIBERS

Tensile test was performed to the model with above-mentioned dimensions. The test was done with one edge fixed and giving 1% length elongation towards opposite edge. The results for Young's Moduli, Shear Moduli, and Poisson's ratio is discussed.

Young's Modulus along fiber direction.

Table 2: Young's Modulus for different fiber volume percentage and aspect ratio.

ASPECT RATIO(L/D)	E_z(GPa) for 5%	E_z(GPa) for 10%	E_z(GPa) for 15%	E_z(GPa) for 18%
0	2.865	2.865	2.865	2.865
10	4.503302	5.413111	7.169869	7.183791
20	5.277621	8.985278	11.65906	12.21294
30	8.70628	13.17123	16.41242	17.63791
40	8.866212	14.46023	20.20505	23.66639
60	11.18575	17.04254	21.13602	27.77168
80	11.59276	20.15122	30.32463	35.20425
100	13.72244	22.50158	33.4151	38.0722

Table 2 shows the Young's Modulus for different volume percentage of fiber (5%, 10%, 15% and 18%) up to aspect ratio of 100. At 0 aspect ratio Young's Modulus of the DiF reinforced composite was same as matrix, which was 2.865 GPa. As the aspect ratio of fiber was increased, the Young's Modulus also increased and as the volume percentage of fiber went from 5% to 18%, the Young's Modulus had increased. Further, we also saw,

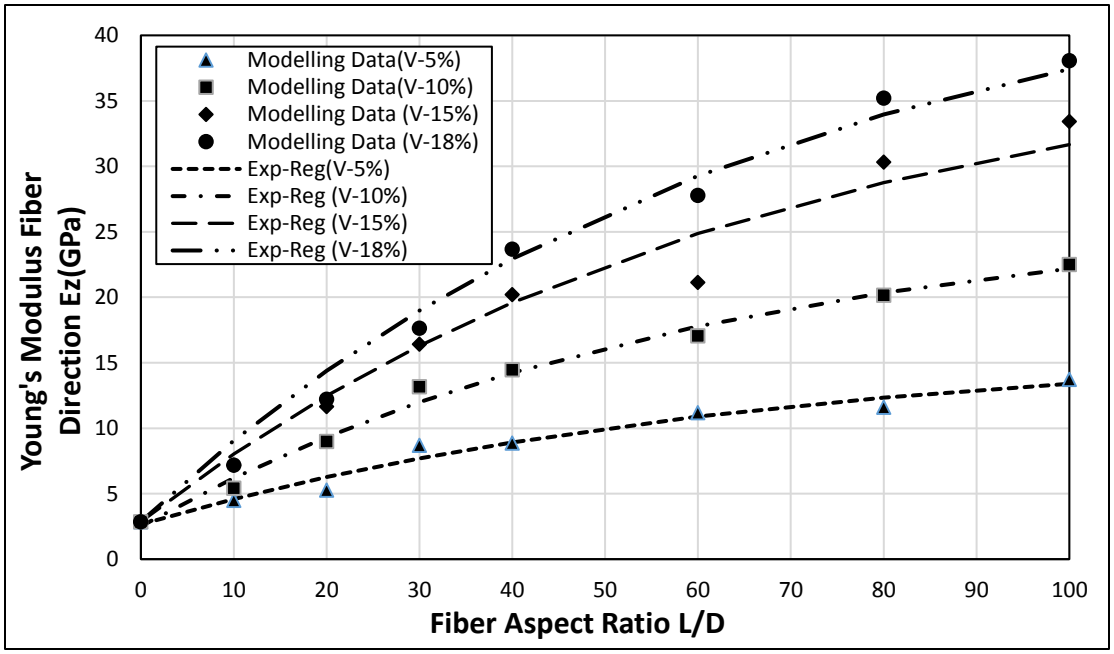

Figure 14: Young's Modulus along fiber direction vs. Fiber aspect ratio up to 100 L/D.

what was the relation of fiber aspect ratio to Young's Modulus and volume of fiber to Young's Modulus. Table 2 data was used to plot figure 1

Here we tried to predict the material behavior of Discontinuous fiber reinforced composites by computer modeling technique. Figure 14 shows the Young's Modulus of discontinuous fiber reinforced composites, along the fiber direction, vs fiber aspect ratio up to 100 L/D. The data from simulations i.e. table 2 were plotted which shows that

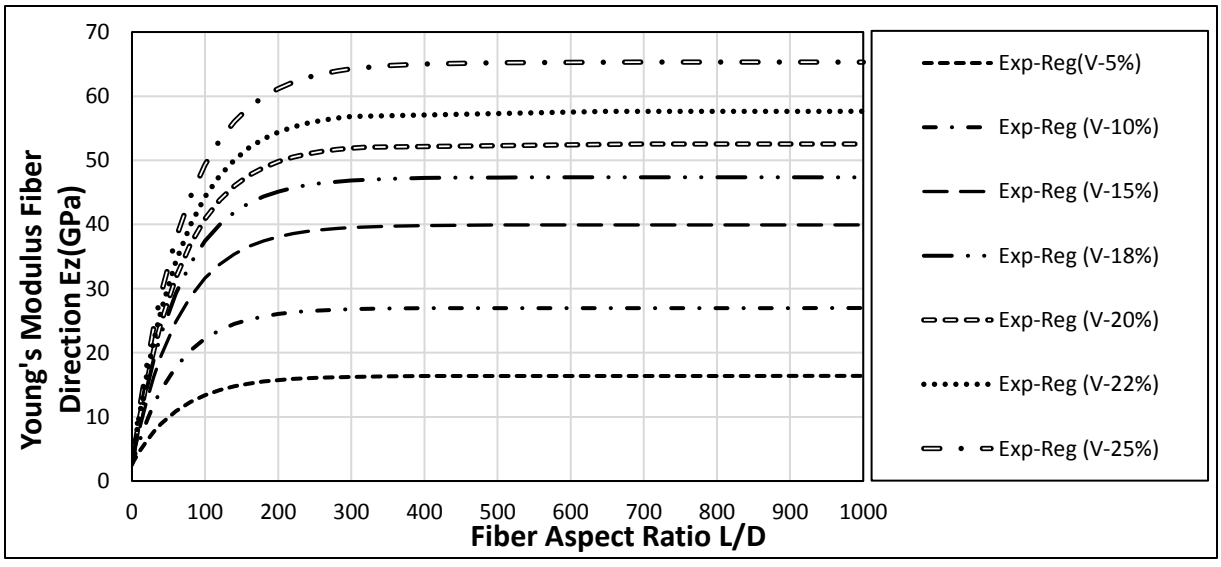

Figure 15: Young's Modulus along fiber direction vs. Fiber aspect ratio up to 1000 L/D.

Young's modulus increases exponentially as the aspect ratio was increased and when the volume percentage (5%, 10%, 15%, and 18%) increased the Young's modulus also increased.

Figure 15 shows the predicted Young's Modulus of discontinuous fiber reinforced composites, along fiber direction, vs fiber aspect ratio up to 1000 L/D and volume percentage of fiber up to 25%. These exponential curves were drawn using regression technique where the data from the simulation was utilized. The exponential curves show that there is sharp increment of Young's modulus up to 300 L/D after that the increment was very slow up to 1000 L/D. Figure 15 shows the prediction of Young's Modulus with different volume percentages (5%, 10%, 15%, 18% ,20%,22%and 25%).

The following equation can be used to predict the Young's Modulus along t fiber direction for different volume percentage and aspect ratios.

$$\mathrm{E_z} = 1.5049 + 2.5519\mathrm{V} + \ (0.589 - 2.5062\mathrm{V}e^{(-0.0178+0.000175\mathrm{V})\mathrm{X}.}$$

Where,

EZ=Young's Modulus along fiber direction.

V=Fiber volume percentage in a composite.

X=Aspect ratio (L/D) of a fiber.

Young's Modulus along fiber transverse direction.

Table 3: Young's Modulus along fiber transverse direction for 5% fiber volume.

ASPECT RATIO(L/D)	E_x for 5%	$E_y$for 5%	AVG
0	2.865	2.865	2.865
5	3.067277	3.072489	3.069883
10	3.221991	3.014215	3.118103
15	3.233881	3.219486	3.226683
20	3.22909	3.224136	3.226613
30	3.26732	3.25701	3.262165
40	3.281774	3.271274	3.276524
60	3.296541	3.300916	3.298729
80	3.301727	3.306475	3.304101
100	3.368444	3.351937	3.36019

Table 4: Young's Modulus along fiber transverse direction for 10% fiber volume.

ASPECT RATIO(L/D)	E_x for 10%	$E_y$for 10%	AVG
0	2.865	2.865	2.865
5	3.163296	3.182486	3.172891
10	3.300624	3.303488	3.302056
15	3.341488	3.334258	3.337873
20	3.356434	3.37734	3.366887
30	3.39011	3.397831	3.393971
40	3.416369	3.396517	3.406443
60	3.471278	3.467981	3.46963
80	3.461668	3.446994	3.454331
100	3.496946	3.499946	3.498446

Table 5: Young's Modulus along fiber transverse direction for 15% fiber volume.

ASPECT RATIO(L/D)	E_x for 15%	E_y for 15%	AVG
0	2.865	2.865	2.865
5	3.285806	3.278155	3.28198
10	3.409424	3.42403	3.416727
15	3.451246	3.459235	3.45524
20	3.492317	3.497119	3.494718
30	3.513008	3.513191	3.5131
40	3.51993	3.515398	3.517664
60	3.557372	3.554259	3.555815
80	3.572629	3.57494	3.573785
100	3.589062	3.596452	3.592757

Table 6: Young's Modulus along fiber transverse direction for 18% fiber volume.

ASPECT RATIO(L/D)	E_x for 18%	E_y for 18%	AVG
0	2.865	2.865	2.865
5	3.381758	3.392479	3.387119
10	3.473231	3.472609	3.47292
15	3.487246	3.488148	3.487697
20	3.56911	3.592206	3.580658
30	3.593231	3.583178	3.588205
40	3.588128	3.593614	3.590871
60	3.603231	3.606997	3.605114
80	3.626447	3.635518	3.630983
100	3.654854	3.64307	3.648962

Table 3, 4, 5 and 6 shows the modelling and simulation data for Young's Modulus for fiber transverse direction at 5%, 10%, 15% and 18% fiber volume respectively. Considering fiber direction as Z, Young's modulus along fiber transverse directions E_y and E_x are very close, which shows our model, is working correctly.

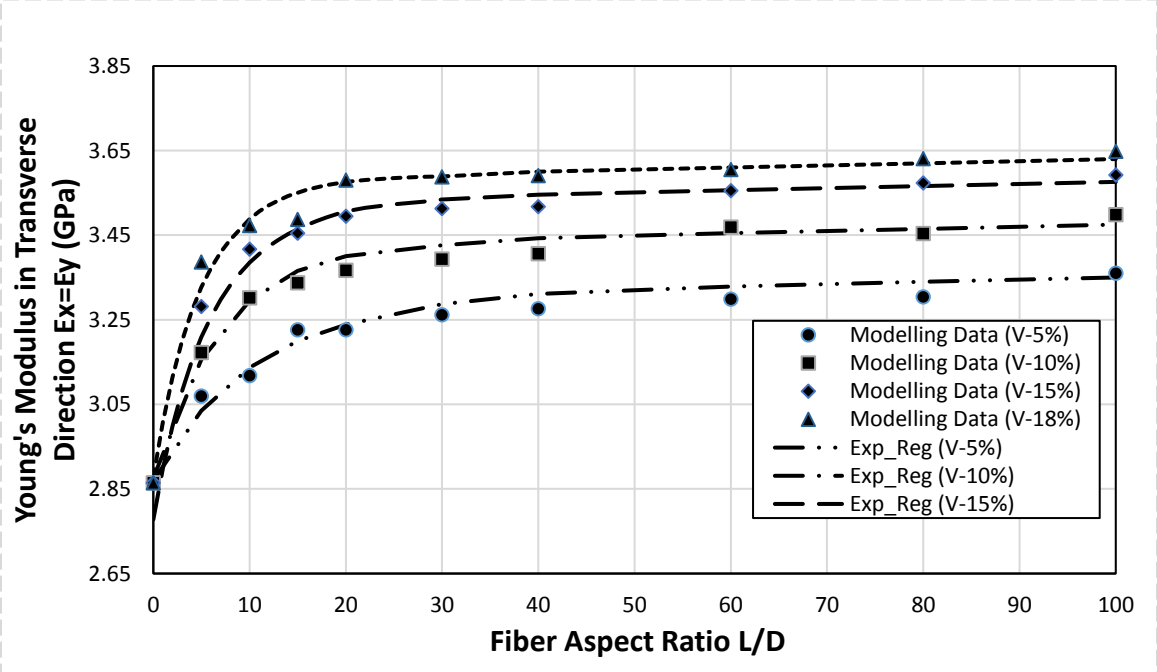

Figure 16: Young's Modulus along fiber transverse direction vs. Fiber aspect ratio up to 100 L/D.

Figure 16 shows the Young's Modulus along transverse direction where each point are average Young's Modulus along Y direction and X direction. From the simulation data, we saw Young's Modulus for both the transverse directions were very close which showed our model was logical. Young's Modulus along the fiber transverse direction was increased exponentially and with increase of fiber volume percentage Young's modulus was also increasing.

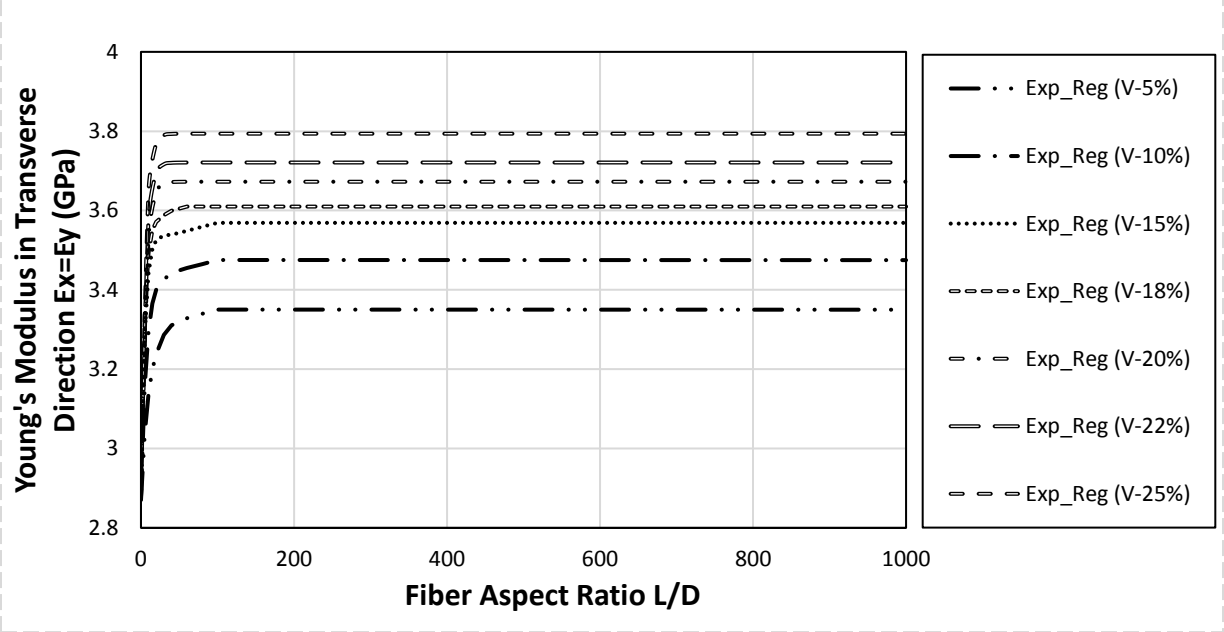

Figure 17: Young's Modulus along fiber transverse direction vs. Fiber aspect ratio up to 1000 L/D.

In figure 17, we can see the regression line extended up to aspect ratio 1000 and volume percentage of fiber up to 25%. Young's Modulus in transverse direction had sharp increment up to around aspect ratio of 60 after that the increment was very less. As the volume percentage of fiber was increase from 5% to 18%, Young's Modulus was also increased. Exponential regression was used to predict the Young's Modulus for more fiber volume percentage like 22%, 25% and so on.

The following equation can be used to predict the Young's Modulus along transverse for different volume percentage and aspect ratios.

$$E_x = E_y = 3.16 + 0.0242V + (-0.3772 - 0.0184V)e^{(-0.1338-0.00176V)X.}$$

Where,

EX=Young's Modulus along fiber transverse direction.

EY= Young's Modulus along fiber transverse direction.

V=Fiber volume percentage in a composite.

X=Aspect ratio (L/D) of a fiber.

Shear Modulus

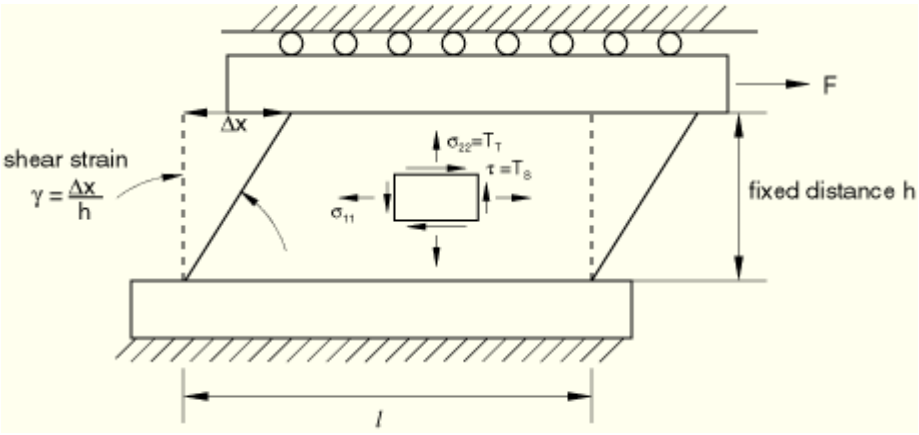

Figure 18: Schematics of Shear test.

Shear test was done using computer modeling technique in order to predict Shear Modulus of discontinuous fiber reinforced composite. We fixed one edge of the model and 1% length displacement was given to other edge. The elongation created strain in the model, which was calculated in order to find force. The displacement for fixed edge was zero in all directions.

Shear Modulus $G_{xy} = G_{yx}$

Table 7: Averaged Shear Modulus along XY and YX plane from modeling.

ASPECT RATIO(L/D)	$G_{xy} = G_{yx}$(GPa) for 5%	$G_{xy} = G_{yx}$(GPa) for 10%	$G_{xy} = G_{yx}$(GPa) for 15%	$G_{xy} = G_{yx}$(GPa) for 18%
1	0.896741	0.901145	0.89564	0.89042
10	0.923984	0.940747	0.965421	0.983718
20	0.956392	0.97583	1.005332	1.027955
30	0.972657	0.994146	1.028599	1.051651
40	0.990592	1.008607	1.045544	1.06978
60	1.004862	1.023849	1.063055	1.09152
80	1.017613	1.035688	1.078927	1.101058
100	1.019472	1.036045	1.084452	1.102917

Table 7 shows the shear modulus of our model with different aspect ratios of fiber (from 1 to 100). Volume percentage of fiber was initially taken 5% which was increased up to 18% .As the volume percentage increased the shear modulus was also increased. Table 7 data was used to plot graph in figure 19.

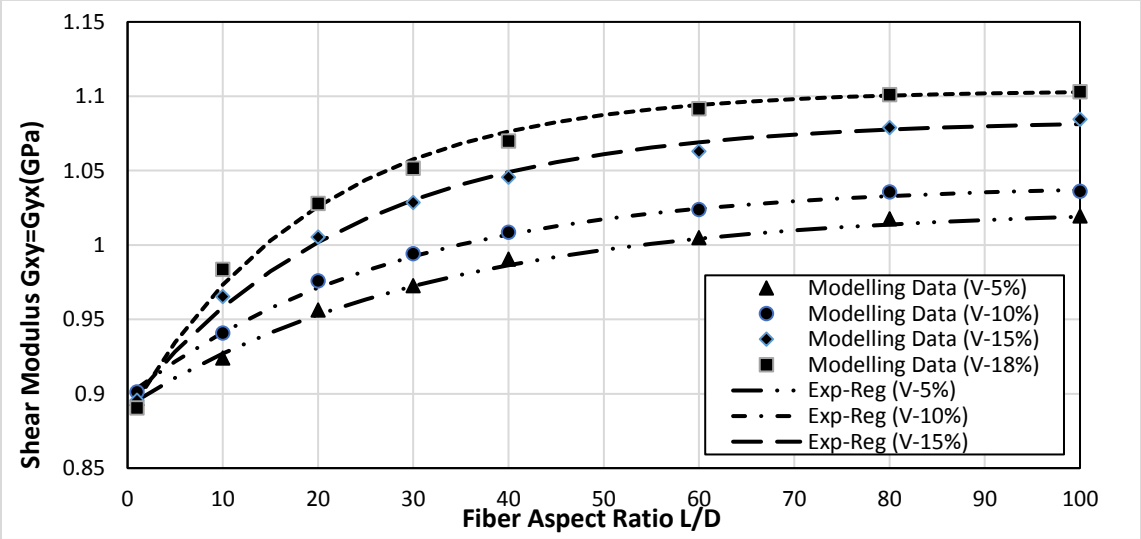

Figure 19: Shear Modulus,$G_{xy} = G_{yx}$ Vs aspect ratio up to 100.

To get the accurate result three panes were chosen along XY plane at 0.4, 0.6 and 0.5 of length and 1 percentage length displacement was given for each plane individually and

the average was taken. As from our simulation result, we found the shear along XY and YX were very close so again the average was taken to plot the graph. Figure 19 shows Shear Modulus along XY plane, which was equal to YX plane. We can clearly say that there is exponential relation between Shear modulus and aspect ratio. As the aspect ratio of fiber increases the Shear Modulus increases and shear, modulus also increases as the volume percentage of fiber increases.

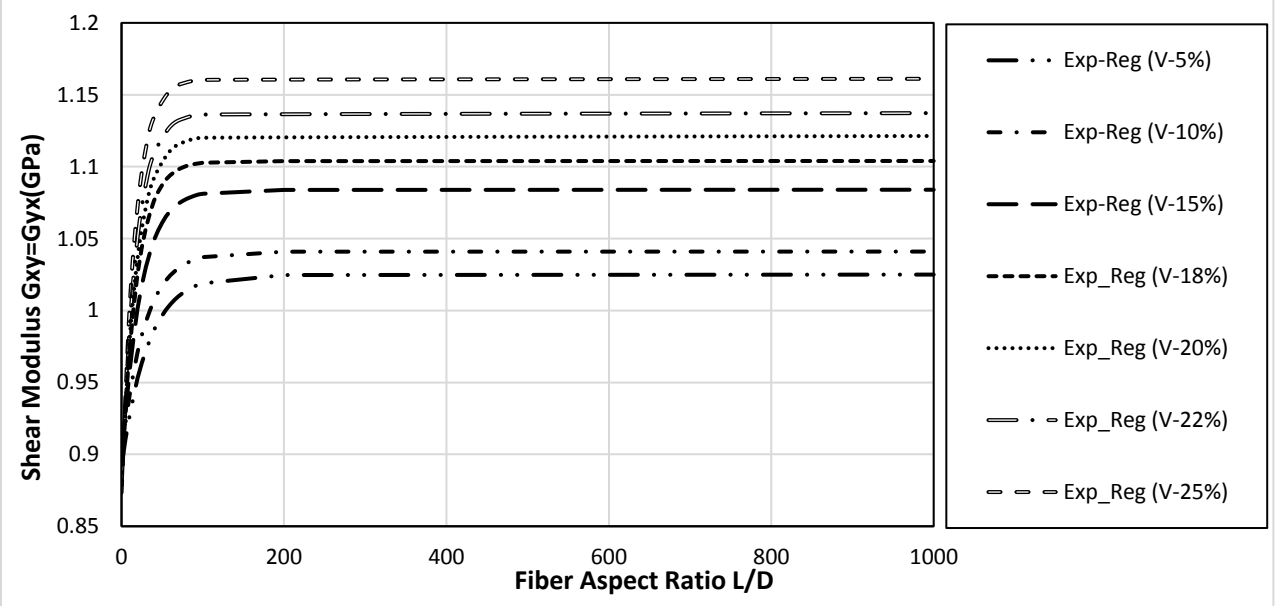

Figure 20: Shear Modulus, $G_{xy} = G_{yx}$, Vs aspect ratio up to 1000.

Figure 20 shows the prediction of Shear Modulus up to 1000 aspect ratio of fiber made by drawing regression line from simulation data. Shear modulus has significant increment up to around 150 aspect ratios of fiber.

The following equation can be used to predict the Shear Modulus along XY plane.

$$\mathrm{G_{xy}} = \mathrm{G_{yx}} = 0.9878 + 0.00631\mathrm{V} + (-0.0896 - 0.00688\mathrm{V})\mathrm{e}^{(-0.0240-0.00144\mathrm{V})\mathrm{X}.}$$

Where,

$\mathrm{G_{xy}}$= Shear Modulus along XY plane.

G_{yx} = Shear Modulus along YX plane.

V=Fiber volume percentage in a composite.

X=Aspect ratio (L/D) of a fiber.

Shear Modulus $G_{yz} = G_{zy} = G_{zx} = G_{xz}$

Table 8: Averaged Shear Modulus along YZ, ZY, XZ and ZX plane from modeling.

ASPECT RATIO(L/D)	$\mathbf{G_{yz} = G_{zy} = G_{zx} = G_{xz}}$**(GPa) for 5%**	$\mathbf{G_{yz} = G_{zy} = G_{zx} = G_{xz}}$**GPa) for 10%**	$\mathbf{G_{yz} = G_{zy} = G_{zx} = G_{xz}}$**GPa) for 15%**	$\mathbf{G_{yz} = G_{zy} = G_{zx} = G_{xz}}$**(GPa) for 18%**
1	0.720101	0.739303	0.787947	0.759162
10	0.923342	0.974045	1.015855	1.064233
20	1.005277	1.074074	1.115963	1.15548
30	1.045157	1.124897	1.156381	1.197402
40	1.078183	1.148982	1.184988	1.223982
60	1.114503	1.167707	1.204914	1.23534
80	1.132239	1.170414	1.221628	1.24432
100	1.129747	1.186726	1.227853	1.25421

Table 8 shows the shear modulus along YZ or ZY or XZ or ZX plane from modelling data, which was used to plot graph 21 to predict the relation of shear modulus with aspect ratio and volume percentage of fiber.

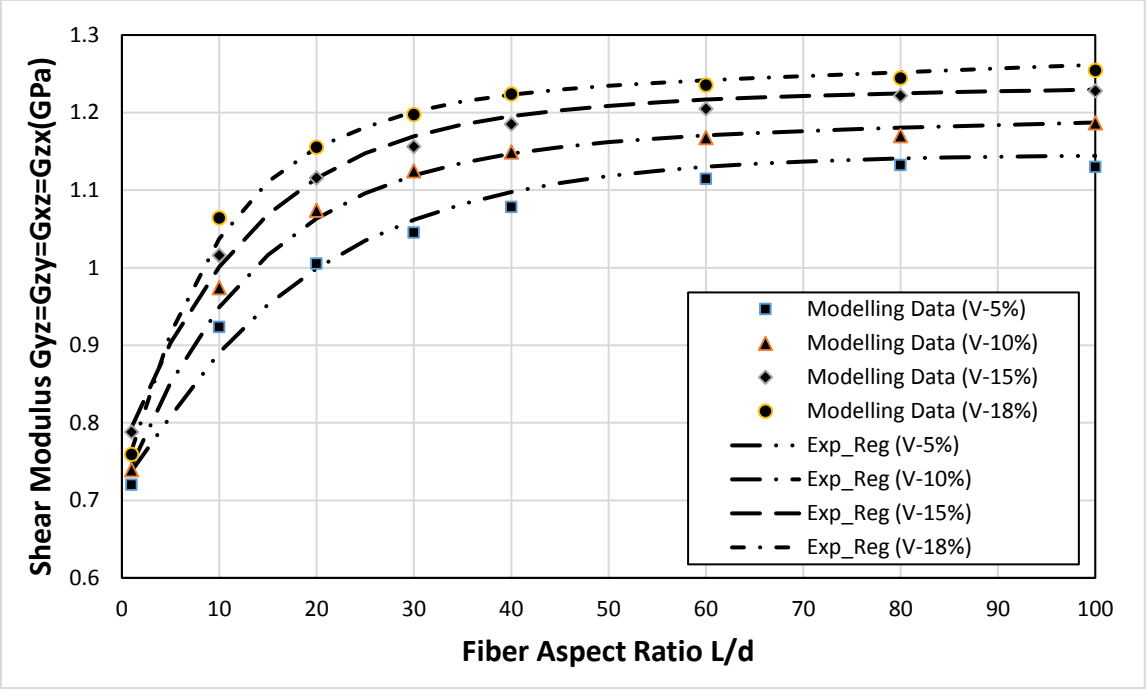

Figure 21: Shear Modulus,$G_{yz} = G_{zy} = G_{xz} = G_{zx}$, Vs aspect ratio up to 100.

From figure 21, we can see the exponential relation between shear modulus along yz plane and aspect ratio of the fiber. Here also, to increase accuracy three different planes were chosen and average was done. G_{yz} , G_{zy} ,G_{xz} and G_{zx} ,values were close so again average was done to get the shear modulus. With increased fiber volume percentage, shear modulus also increased. Figure 22 shows the predicted graph of shear modulus vs aspect ratio up to 1000.From figure 21 and 22we can see that shear modulus have significant increment up to aspect ratio 60 after that there is very less increment. After aspect ratio of fiber reached to 100,the shear modulus has no significant change.

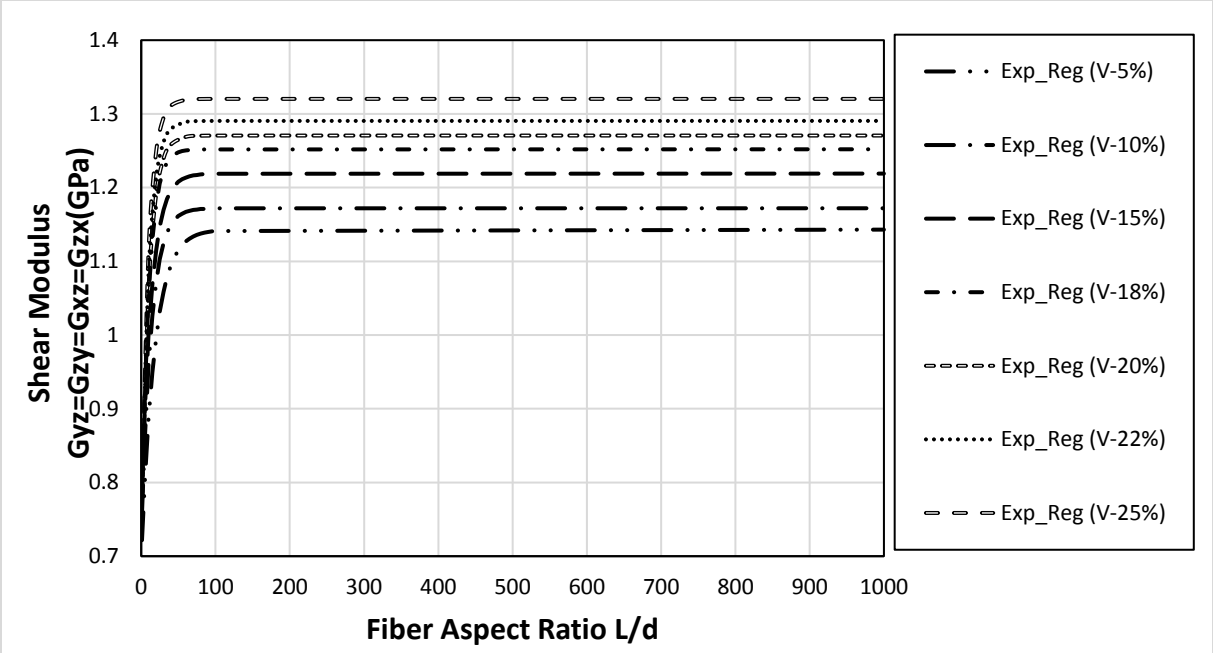

Figure 22: Shear Modulus,$G_{yz} = G_{zy} = G_{xz} = G_{zx}$, Vs aspect ratio up to 1000.

The following equation can be used in order to predict shear modulus along YZ, ZY, XZ and ZX plane.

$$\mathrm{G_{yz}} = \mathrm{G_{zy}} = \mathrm{G_{xz}} = \mathrm{G_{zx}}$$
$$= 1.12702 + 0.00628\mathrm{V} + (-0.4135 - 0.00496\mathrm{V})\mathrm{e}^{(-0.03913-0.00288\mathrm{V})\mathrm{X}.}$$

Where,

$\mathrm{G_{yz}}$ = Shear Modulus along YZ plane.

$\mathrm{G_{zy}}$ = Shear Modulus along ZY plane.

$\mathrm{G_{xz}}$ = Shear Modulus along XZ plane.

$\mathrm{G_{zx}}$ = Shear Modulus along ZX plane.

V=Fiber volume percentage in a composite.

X=Aspect ratio (L/D) of a fiber

Poisson's Ratio

Poisson's ratio $\mathrm{v_{xz}} = \mathrm{v_{yz}}$

Table 9: Poisson's ratio $v_{xz} = v_{yz}$ from modelling.

ASPECT RATIO(L/D)	$v_{xz} = v_{yz}$ (for V- 5%)	$v_{xz} = v_{yz}$ (for V- 10%)	$v_{xz} = v_{yz}$ (for V- 15%)	$v_{xz} = v_{yz}$ (for V- 18%)
0	0.36	0.36	0.36	0.36
10	0.26329	0.20028	0.14898	0.13643
20	0.19506	0.12701	0.09379	0.07649
40	0.14117	0.09113	0.06714	0.04995
60	0.11955	0.07407	0.05644	0.03864
80	0.11415	0.06165	0.0447	0.02504
100	0.10138	0.05838	0.0428	0.02397

Table 9 shows the modelling data of Poisson's ratio $v_{xz} = v_{yz}$. Poisson's ratio $v_{xz} = v_{yz}$ was decreased as the aspect ratio increases it shows there was less contraction in transverse direction, which shows more stability of a model under tensile load. As the volume percentage of fiber increases the Poisson's ratio, $v_{xz} = v_{yz}$ decreases which shows the model becomes more stable as volume of fiber increases with less contraction in transverse direction.

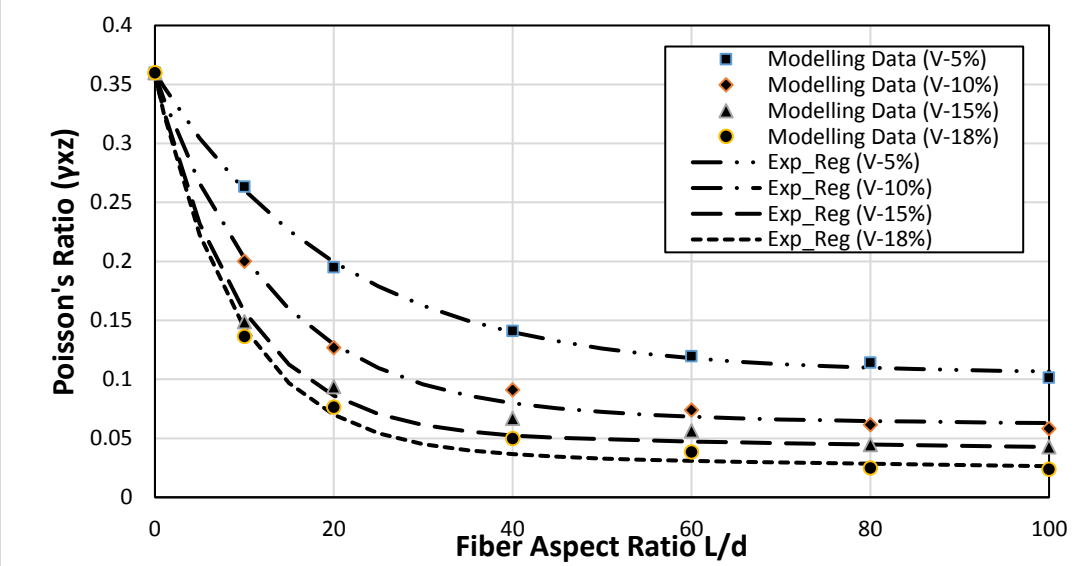

Figure 23: Poisson's ratio $v_{xz} = v_{yz}$ up to aspect ratio 100.

Figure 23 shows the graph between Poisson's ratios, $v_{xz} = v_{yz}$ vs. aspect ratio of a fiber. The graph was plotted from the table 10 modelling data, which showed there was exponential relation between Poisson's ratio, $v_{xz} = v_{yz}$ and fiber aspect ratio .As the aspect ratio of fiber increased the Poisson's ratio, $v_{xz} = v_{yz}$ decreased , and as the volume percentage of fiber increased the Poisson's ratio, $v_{xz} = v_{yz}$ decreased. Figure 24 shows the graph between Poisson's ratio, $v_{xz} = v_{yz}$ and aspect ratio of fiber up to 1000 and volume percentage of fiber up to 25%, which was developed by regression function. As the aspect ratio of fiber increased above 200 there was very less decrement of Poisson's ratio, $v_{xz} = v_{yz}$.

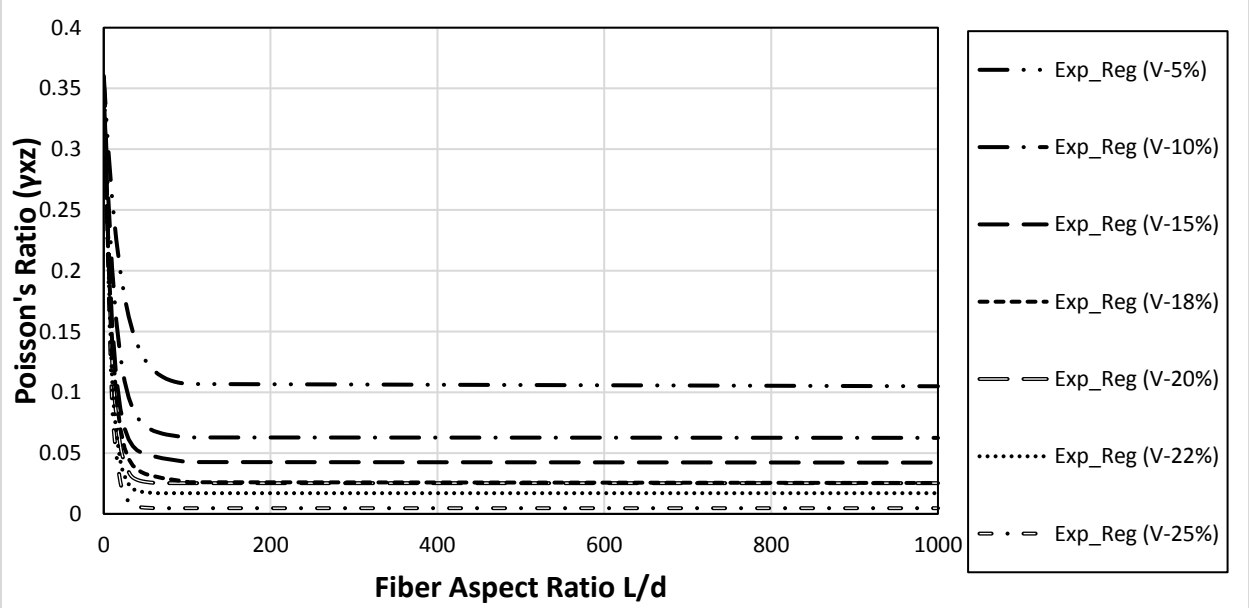

Figure 24: Poisson's ratio $v_{xz} = v_{yz}$ up to aspect ratio 1000.

Following equation can be used to predict Poisson's ratio, $v_{xz} = v_{yz}$ with different aspect ratio and volume percentage.

$$v_{xz} = v_{yz} = 0.1275 + 0.0054V + (0.23328 + 0.005256V)e^{(-0.02808-0.00471V)X.}$$

Where,

$\nu_{xz} = \nu_{yz}$ = Poisson's ratios.

V=Fiber volume percentage in a composite.

X=Aspect ratio (L/D) of a fiber.

Poisson's ratio $\nu_{xy} = \nu_{yx}$

Table 10: Poisson's ratio $\nu_{xy} = \nu_{yx}$ from modelling

ASPECT RATIO(L/D)	$\nu_{xy} = \nu_{yx}$ (for V- 5%)	$\nu_{xy} = \nu_{yx}$ (for V- 10%)	$\nu_{xy} = \nu_{yx}$ (for V- 15%)	$\nu_{xy} = \nu_{yx}$ (for V- 18%)
0	0.36	0.36	0.36	0.36
10	0.38603	0.40028	0.41014	0.4281
20	0.42863	0.43947	0.44606	0.45437
40	0.45727	0.47099	0.4809	0.4871
60	0.46992	0.4806	0.4908	0.5092
80	0.47252	0.48979	0.5051	0.5109
100	0.47798	0.50066	0.5106	0.517056

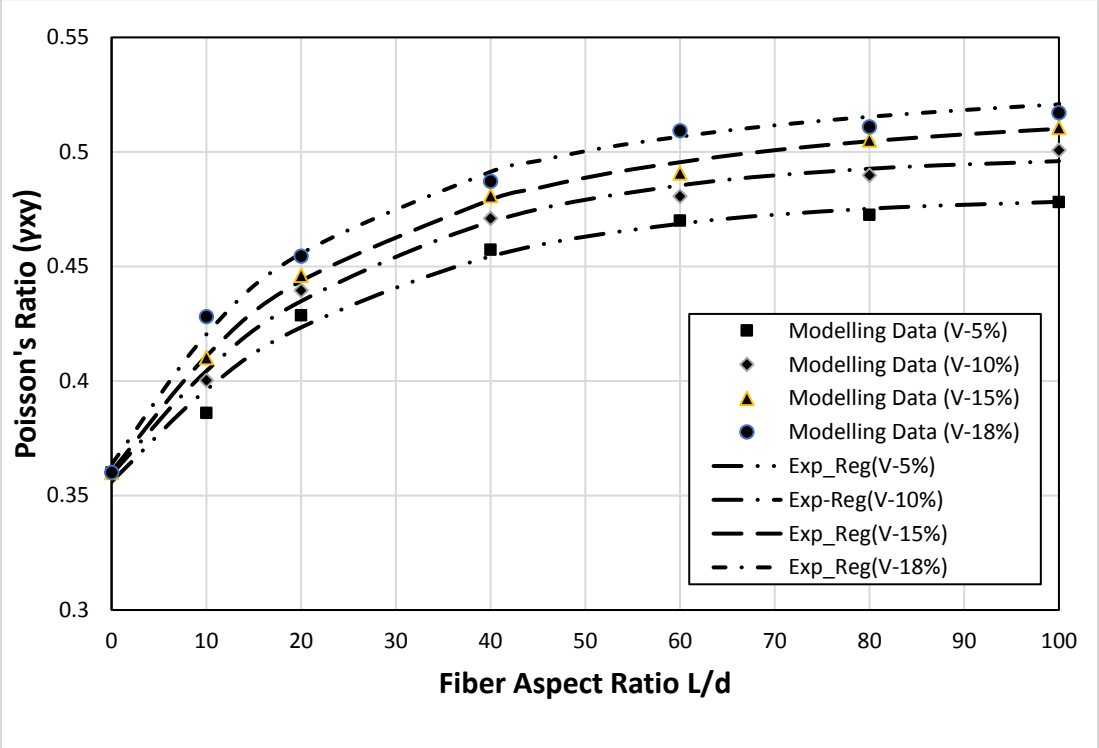

Figure 25: Poisson's ratio $\nu_{xy} = \nu_{yx}$ up to aspect ratio 100.

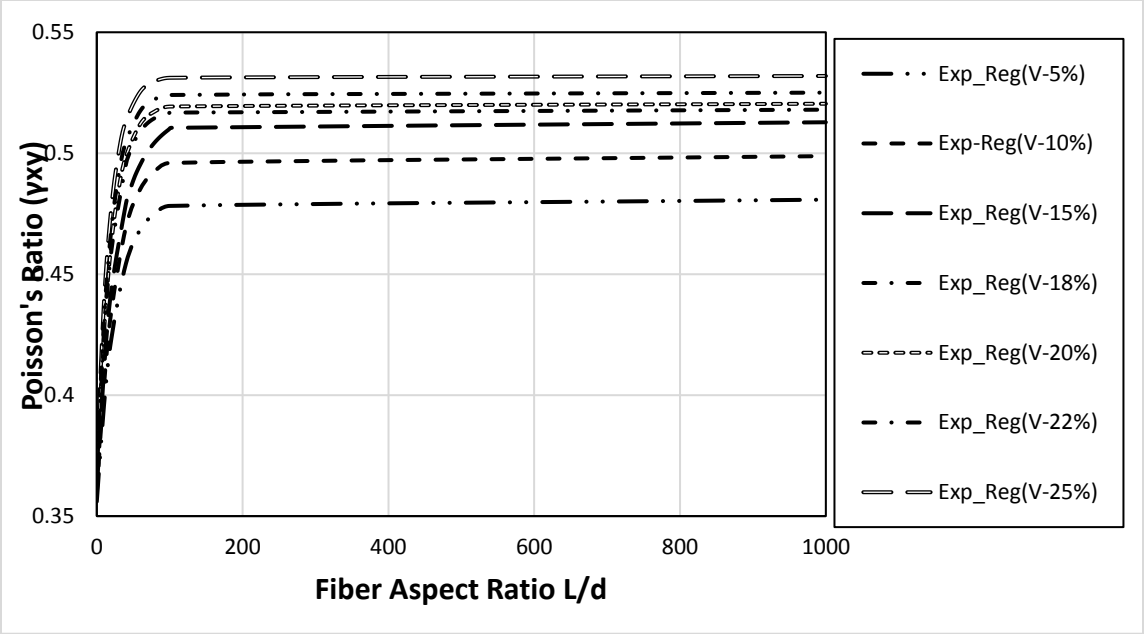

Figure 26: Poisson's ratio $\mathrm{v}_{xy} = \mathrm{v}_{yx}$ *up to aspect ratio 1000.*

Table 10 shows the modelling data of Poisson's ratio, $\mathrm{v_{xy}} = \mathrm{v_{yx}}$ whereas the aspect ratio of fiber increases there is slight increment in Poisson's ratio, $\mathrm{v_{xy}} = \mathrm{v_{yx}}$. Poisson's ratio, $\mathrm{v_{xy}} = \mathrm{v_{yx}}$ slightly increased with volume percentage of fiber increased. Figure 25 and 26 is the data plot of table 10 which shows there was exponential relation between Poisson's ratio, $\mathrm{v_{xy}} = \mathrm{v_{yx}}$ and aspect ratio.

The following equation can be used to predict Poisson's ratio, $\mathrm{v_{xy}} = \mathrm{v_{yx}}$ with different aspect ratio and volume percentage of fiber.

$$\mathrm{v_{xy}} = \mathrm{v}_{yx} = 0.4687 + 0.00267\mathrm{V} + (-0.1173 - 0.00188\mathrm{V})\mathrm{e}^{(-0.03432-0.00063\mathrm{V})\mathrm{X}.}$$

Where,

$\mathrm{v_{xy}} = \mathrm{v_{yx}}$ = Poisson's ratios.

V=Fiber volume percentage in a composite.

X=Aspect ratio (L/D) of a fiber.

Poisson's ratio $v_{zx} = v_{zy}$

Table 11: Poisson's ratio $v_{zx} = v_{zy}$ from modelling.

ASPECT RATIO(L/D)	$v_{zx} = v_{zy}$**(for V- 5%)**	$v_{zx} = v_{zy}$**(for V- 10%)**	$v_{zx} = v_{zy}$**(for V- 15%)**	$v_{zx} = v_{zy}$**(for V- 18%)**
0	0.36	0.36	0.36	0.36
10	0.35941	0.35869	0.35782	0.3572
20	0.35888	0.357855	0.35682	0.356098
40	0.3574	0.35642	0.35556	0.354551
60	0.35641	0.355185	0.35383	0.3522
80	0.354856	0.35397	0.35252	0.3514
100	0.35363	0.352535	0.35145	0.35076

Table 11 shows the Poisson's ratio, $v_{zx} = v_{zy}$ from modelling data, where Poisson's ratio, $v_{zx} = v_{zy}$ decreased as the aspect ratio of fiber increased. Decrease in Poisson's ratio, $v_{zx} = v_{zy}$ makes our model structurally more stable by less contraction in transverse direction. From table 11 we can see Poisson's ratio, $v_{zx} = v_{zy}$ decreases as the volume percentage of fiber increases which again means with higher volume percentage of fiber the model is more stable with less contraction in transverse direction under tension.

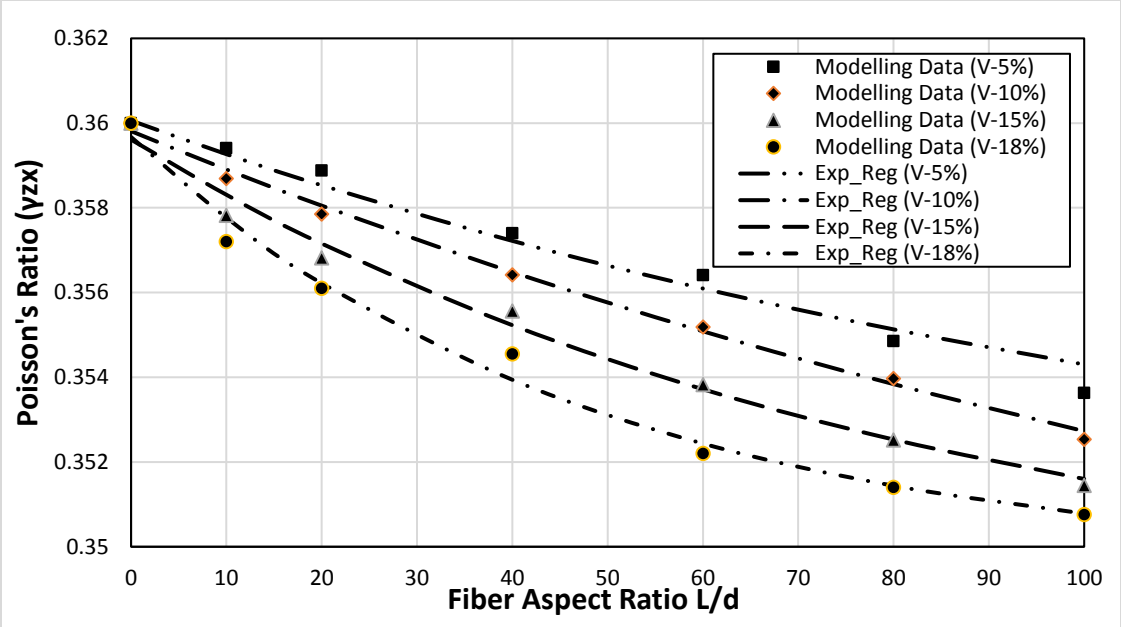

Figure 27: Poisson's ratio $v_{zx} = v_{zy}$ *up to aspect ratio 100.*

Figure 27 shows the graph plotted with modelling data for Poisson's ratio, $v_{zx} = v_{zy}$,where there is exponential relation between Poisson's ratio, $v_{zx} = v_{zy}$ and aspect ratio of fiber. With the increase of fiber aspect ratio Poisson's ratio, $v_{zx} = v_{zy}$ decrease and with increase of volume percentage of fiber Poisson's ratio, $v_{zx} = v_{zy}$decreases. Figure 28 shows the graph from regression equation for Poisson's ratio, $v_{zx} = v_{zy}$ vs aspect ratio of fiber up to 25% volume of fiber.

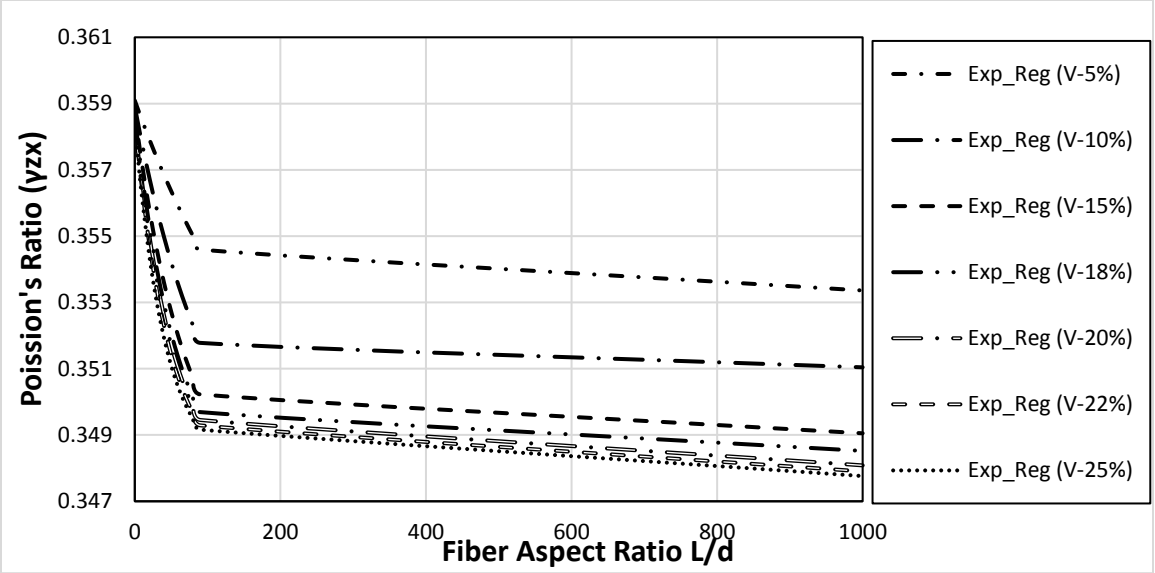

Figure 28: Poisson's ratio $\nu_{zx} = \nu_{zy}$ *up to 25% volume of fiber.*

The following equation can be used to predict Poisson's ratio, $\nu_{zx} = \nu_{zy}$ with different aspect ratio and volume percentage of fiber.

$$\nu_{zx} = \nu_{zy} = 0.3465 + 9.49e-5V + (-0.01367 - 0.00013)e^{(-0.000137-0.00097V)X.}$$

Where,

$\nu_{zx} = \nu_{zy}$ = Poisson's ratios.

V=Fiber volume percentage in a composite.

X=Aspect ratio (L/D) of a fiber.

4.2 3D Model

For 3D model, we used two-step approach to find material property of discontinuous fiber reinforced composite. In first step uniaxial 1D fiber were generated and tensile, shear test by computer modelling was done to find the material property like Young's Modulus, Shear Modulus and Poisson's ratio. In second step, a 3D model of discontinuous fiber reinforced composite was made where each element represented an element of

composites reinforced with unidirectional randomly oriented fibers. In order to find the material property tensile, shear test was done by computer modelling for 3D model of discontinuous fiber reinforced composite.

Young's Modulus.

Table 12: Young's Modulus of 3D model with different fiber volume percentage and aspect ratio.

ASPECT RATIO(L/D)	E(GPa) for 5%	E(GPa) for 10%	E(GPa) for 15%	E(GPa) for 18%
1	2.895711	2.905743	2.928782	2.941714
10	3.028235	3.266615	3.511004	3.622074
20	3.231815	3.579946	4.168037	4.334126
40	3.786791	4.427269	4.960142	5.325189
60	4.080212	4.682713	5.179204	5.586043
80	4.146875	4.885792	5.683234	6.041571
100	4.350898	5.134529	6.019687	6.214202

Table 12 shows the Young's Modulus for different volume percentage and aspect ratio of fiber. Young's Modulus was increased as the aspect ratio of fiber increased and as the volume percentage (5%, 10%, 15% and 20%) of fiber increased Young's Modulus increased.

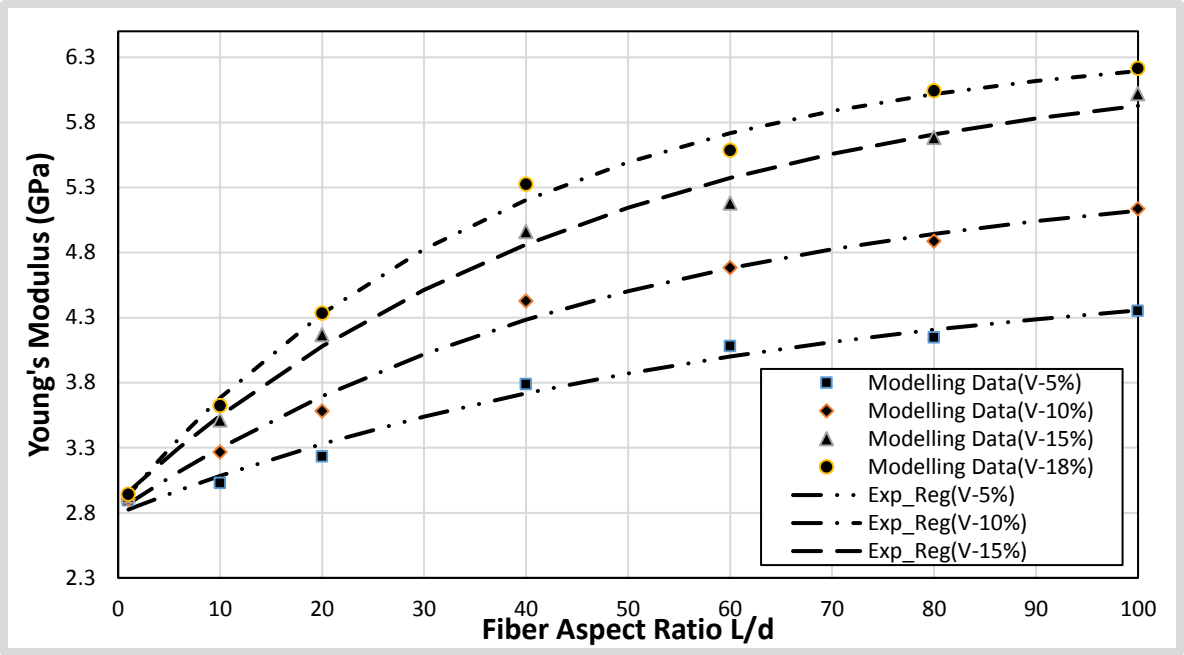

Figure 29: Young's Modulus of 3D model, along fiber direction vs. Fiber aspect ratio up to 100 L/D.

Figure 29 is the graph between Young's Modulus vs. aspect ratio of fiber up to 100 L/D. There is exponential relation between Young's Modulus and aspect ratio of fiber, where Young's Modulus of a discontinuous fiber reinforced composite increases as the aspect ratio of fiber increases. As volume percentage (5%, 10%, 15% and 20%) of fiber increases Young's Modulus also increases. Using the regression function, it was possible to predict Young's Modulus of 3D model which is shown in figure 30, where there was sharp increment of Young's Modulus around aspect ratio of 200 above aspect ratio of 200 there was just little change in Young's Modulus.

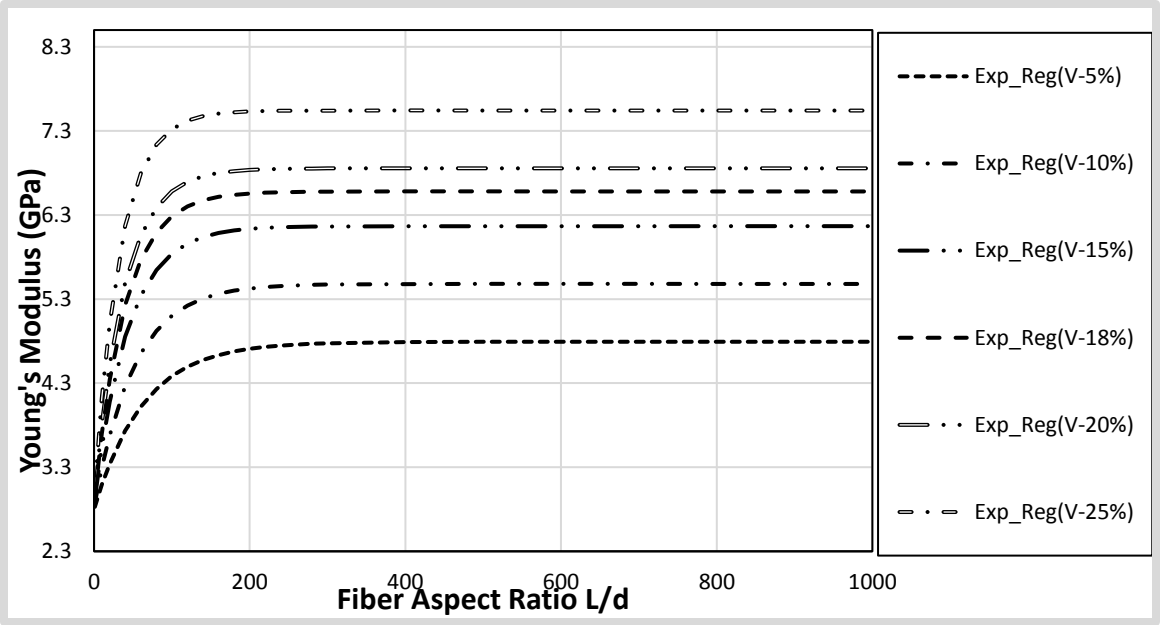

Figure 30: Predicted Young's Modulus of 3D model along fiber direction vs. Fiber aspect ratio up to 1000 L/D.

The following equation can be used to predict the Young's Modulus of a discontinuous fiber reinforced composite with different volume percentage and aspect ratios.

$$E = 4.105 + 0.1357V + (-1.3333 - 0.13233V)e^{(-0.0122-0.00073V)X.}$$

Where,

E=Young's Modulus.

V=Fiber volume percentage in a composite.

X=Aspect ratio (L/D) of a fiber.

Shear Modulus

Shear test was done in order to find Shear Modulus of discontinuous fiber reinforced composite. The set up for shear test was done as in 1D where one edge of cuboid model was kept fixed and opposite edge was given 1% of length deformation. Three planes at 0.2-0.4,0.4-0.6,0.6-0.8 of length were deformed respectively and average shear modulus taken in order to obtain high accuracy.3D model being symmetrical, shear modulus in all planes i.e. $G_{xy} = G_{yx}$, $G_{yz} = G_{zy}$,and $G_{zx} = G_{xz}$ are very close so average shear modulus was done.

Table 13: Averaged Shear Modulus for 3D model.

ASPECT RATIO(L/D)	G (GPa) for 5%	G (GPa) for 10%	G (GPa) for 15%	G (GPa) for 18%
1	1.089358	1.080824	1.118298	1.142424
10	1.106013	1.177239	1.266408	1.317129
20	1.182846	1.29637	1.524502	1.581764
40	1.332672	1.514571	1.75579	1.935635
60	1.473552	1.671239	1.872133	2.029874
80	1.476272	1.800807	2.047707	2.25051
100	1.557127	1.86609	2.164207	2.339338

Table 13 shows the shear modulus for 3D model REV of discontinuous fiber reinforced composite. Shear modulus was increased as the fiber aspect ratio increased and increased with volume percentage of fiber. Table 13 data was used to plot graph to know the relation of fiber aspect ratio and volume percentage with shear modulus.

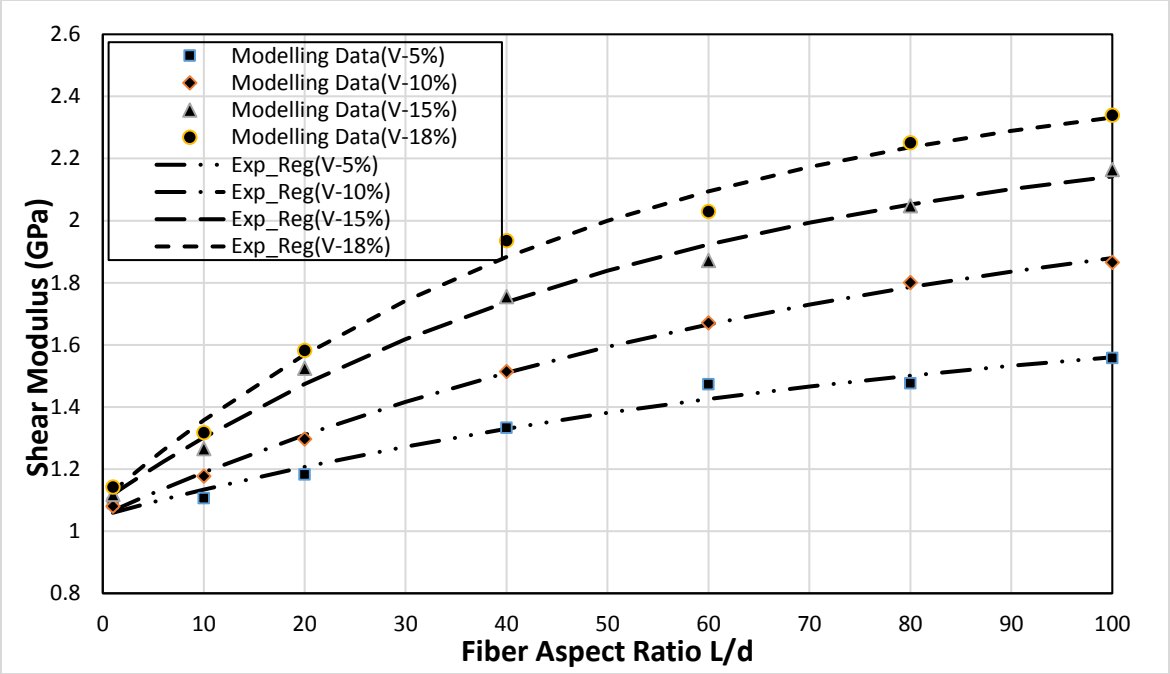

Figure 31: Shear Modulus, G of 3D model Vs aspect ratio up to 100.

Figure 31 shows the shear modulus vs aspect ratio of fiber with different volume percentage of fiber. There was exponential relation between shear modulus and fiber aspect ratio, as the fiber ratio increased shear modulus increased exponentially. Figure 32 shows the prediction of shear modulus up to 1000 aspect ratio of fiber where there was significant increment of shear modulus up to around aspect ratio of 300 after that there was very little increment of shear modulus as the aspect ratio increased up to 1000.

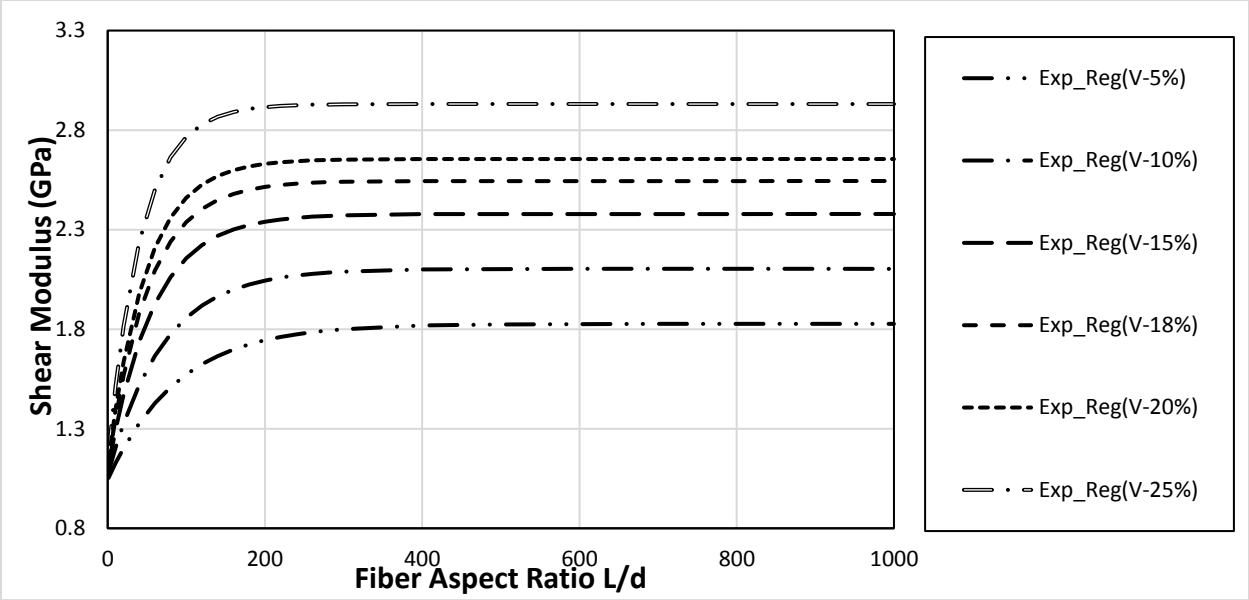

Figure 32: Predicted Shear Modulus, G of 3D model Vs aspect ratio up to 1000.

The following equation can be used to predict the Shear Modulus of a discontinuous fiber reinforced composite with different volume percentage and aspect ratios.

$$G = 1.5508 + 0.055204V + (-0.52867 - 0.05083V)e^{(-0.00811-0.00063V)X.}$$

Where,

G=Shear Modulus.

V=Fiber volume percentage in a composite.

X=Aspect ratio (L/D) of a fiber.

Poisson's ratio

Table 14: Poisson's ratio ν for 3D model.

ASPECT RATIO(L/D)	ν (for V-5%)	ν (for V-10%)	ν (for V-15%)	ν (for V-18%)
0	0.36	0.36	0.36	0.36
10	0.35941	0.35869	0.35782	0.3572
20	0.35888	0.357855	0.35682	0.356098
40	0.3574	0.35642	0.35556	0.354551
60	0.35641	0.355185	0.35383	0.3522

80	0.354856	0.35397	0.35252	0.3514
100	0.35363	0.352535	0.35145	0.35076

Table 14 shows the Poisson's ratio of 3D model form modeling data where, Poisson's ratio decreased as the aspect ratio of fiber increased, and Poisson's ratio again decreased as the fiber volume percentage increased. This decrease in Poisson's ratio shows that less contraction in transverse direction under tension, which increase material stability, so with the fiber aspect ratio and volume percentage of fiber increased the discontinuous fiber reinforced composite stability increased. Figure 33 shows the decrement in Poisson's ratio as the fiber aspect ratio and volume percentage of fiber increased. There was exponential relation between fiber aspect ratio and Poisson's ratio.

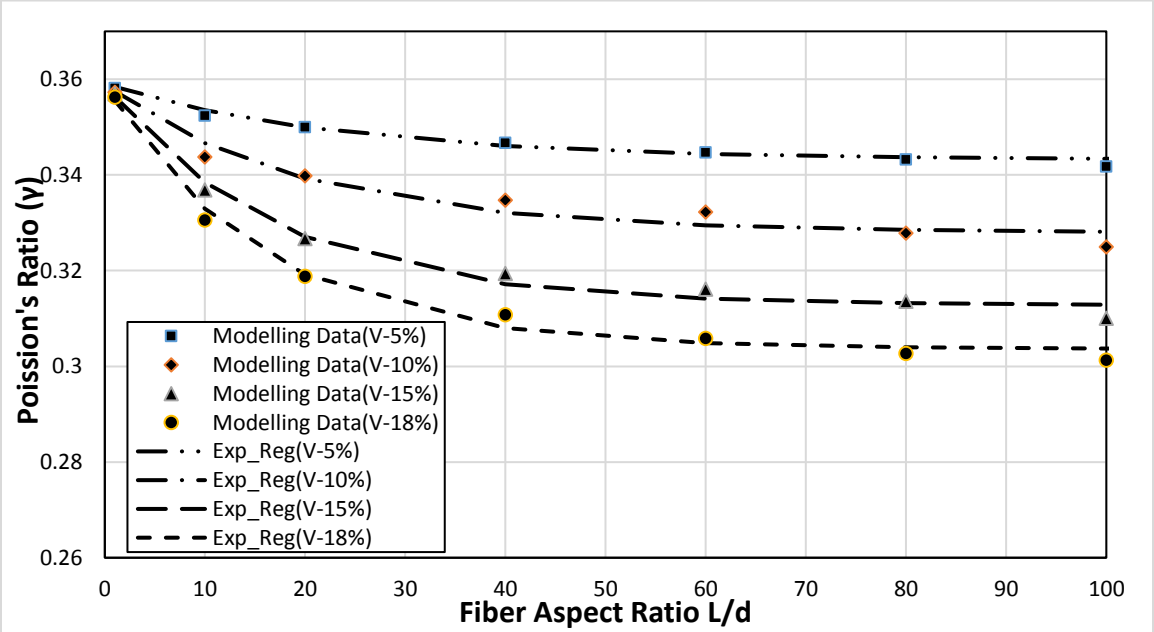

Figure 33: Poisson's ratio ν of 3D model discontinuous fiber reinforced composite up to aspect ratio 100.

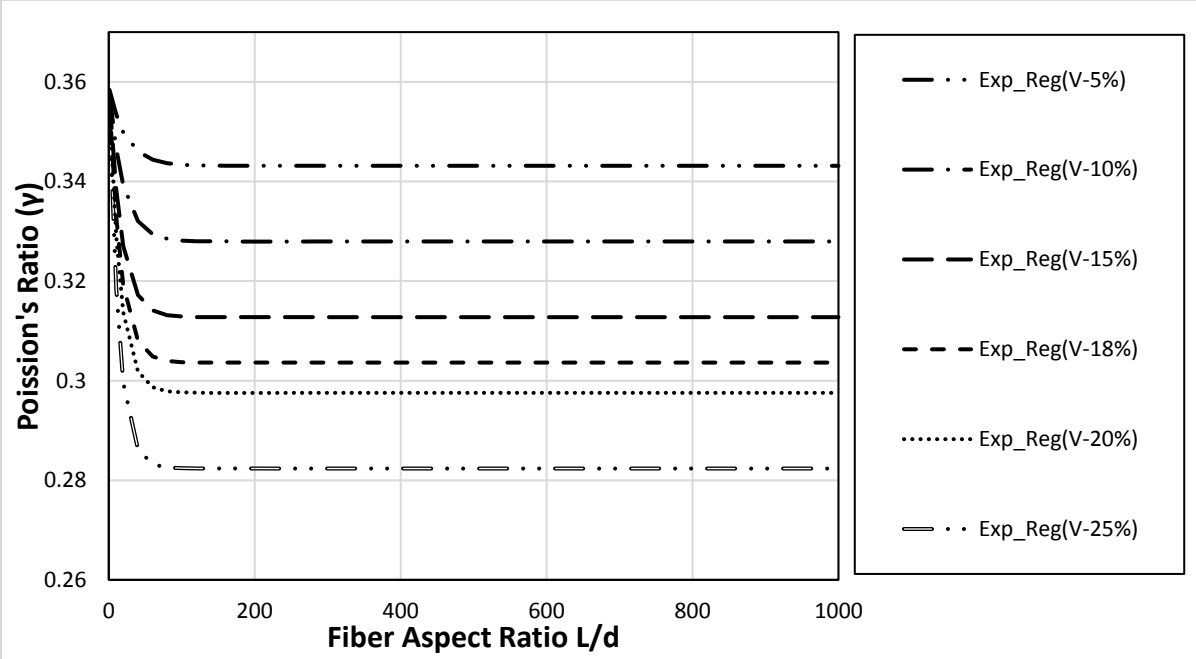

Figure 34: Predicted Poisson's ratio ν of 3D model discontinuous fiber reinforced composite up to aspect ratio 100.

Figure 34 shows the predicted Poisson's ratio of discontinuous fiber reinforced composite up to aspect ratio of fiber 1000. From figure 34 shows the Poisson's ratio decreases significantly up to 100 aspect ratios of fiber after that there is little decrement of Poisson's ratio.

The following equation can be used to predict Poisson's ratio of discontinuous fiber reinforced composite with different aspect ratio and volume percentage of fiber.

$$\nu = 0.35835 - 0.00304V + (0.000779 + 0.003028)\, e^{(-0.03482-0.00159V)X.}$$

Where,

ν = Poisson's ratios.

V=Fiber volume percentage in a composite.

X=Aspect ratio (L/D) of a fiber.

Prediction for 1 D Continuous Fiber Reinforced Composite.

Table 115: Predicted Material Property for continuous fiber reinforced composite.

Vol %	0	5	10	15	20	25
Ez	2.865	14.264	27.023	39.7834	52.542	65.3024
Ex=Ey	2.865	3.16	3.281	3.402	3.523	3.644
Gxy=Gyx	1.053	1.1245	1.173	1.21655	1.2601	1.30365
Gzx=Gxz	1.053	1.41245	1.5137	1.60517	1.6941	1.80365
Vxz=Vyz	0.36	0.1002	0.0572	0.0426	0.0239	0.0237
Vxy=Vyx	0.36	0.469	0.501	0.51	0.511	0.51
Vzx=Vzy	0.36	0.353	0.352	0.351	0.35	0.35

Table 15 shows the predicted material property for continuous fiber reinforced composite. Regression equations was used to for prediction which shows that the material property for discontinuous fiber reinforced composite at higher aspect ratio around 1000 has nearly similar material property as that of continuous fiber reinforced composite.

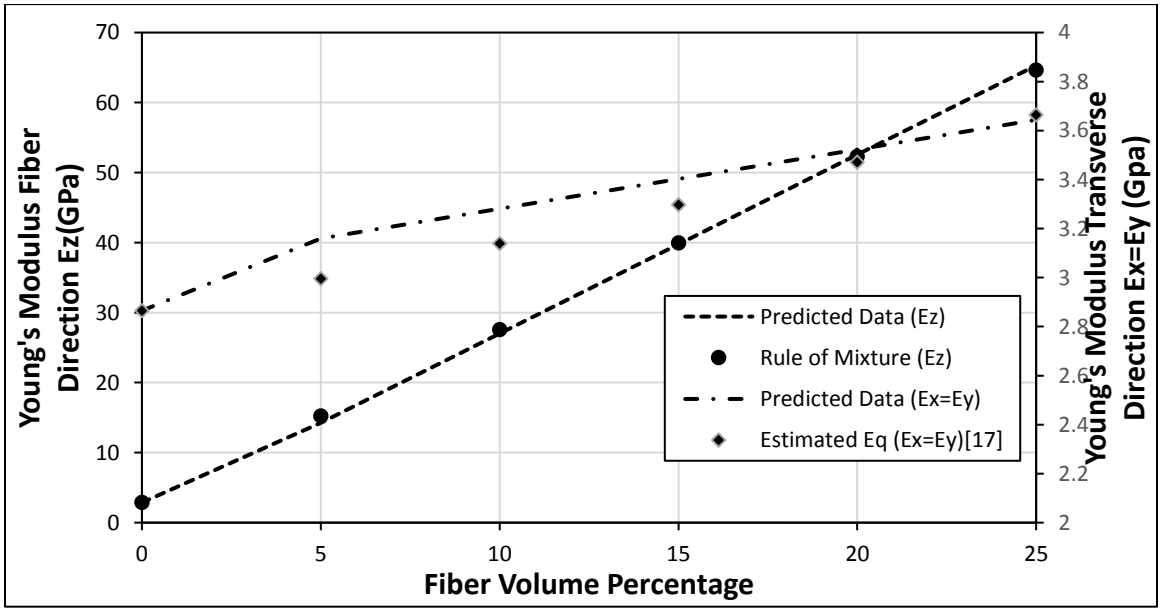

Figure 35: Predicted Young's modulus for continuous fiber reinforced composite model.

Using table 15 Young's modulus for fiber direction and fiber transverse direction was plotted for continuous fiber reinforcement, which is shown in figure 35. Young's modulus increased as the volume percentage of fiber increased for continuous fiber reinforced composite. Furthermore, validation was done using the rule of mixture and prediction equation for fiber direction and fiber transverse direction respectively.

Rule of mixture: $Ez = Vf \times Ezf + Vm \times Em$

Estimated Equation: $Ex = Ey = \frac{Exf \times Em}{Vf \times Em + Vm \times Exf}$

Where,

Ez=Young's Modulus along fiber direction.

Ex = Ey= Young's Modulus along fiber transverse direction.

Vf =Volume of fiber in composite.

Vm = Volume of matrix in composite

Ef = Young's Modulus of fiber.

Em = Young's Modulus of matrix material.

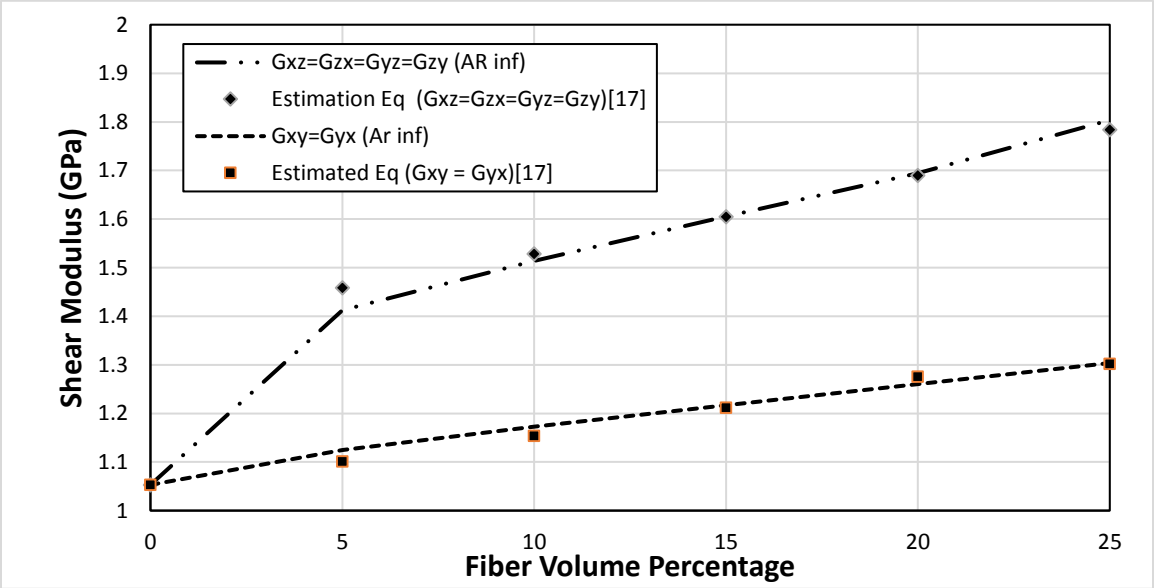

Figure 36: Predicted Young's modulus for continuous fiber reinforced composite model.

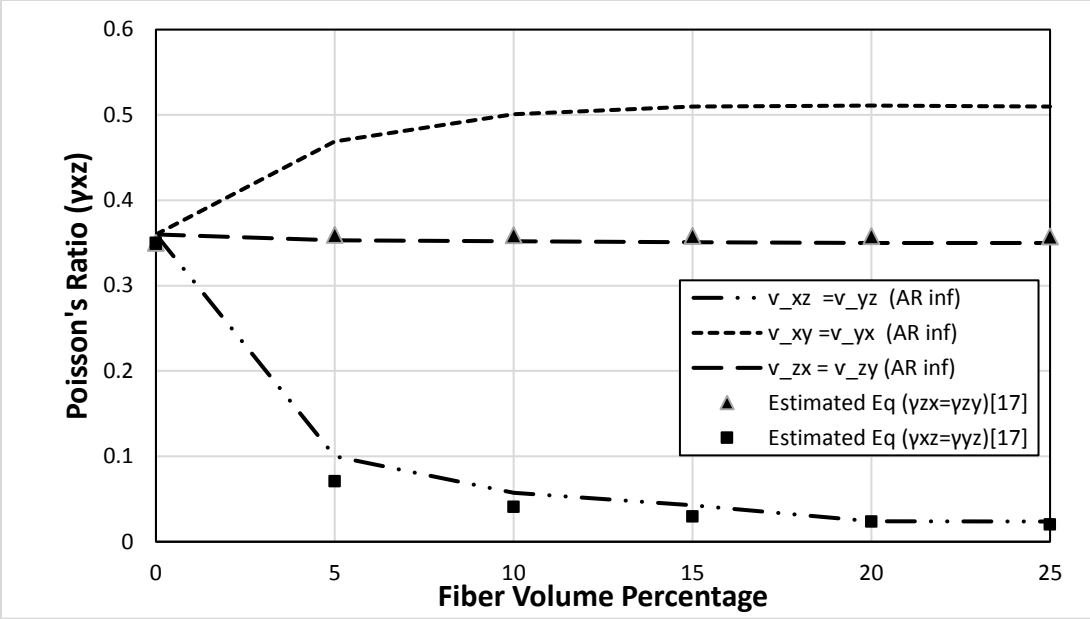

Figure 37: Predicted Poisson's ratio for continuous fiber reinforced composite model.

Using table 15 Shear modulus and Poisson's ratio was drawn for continuous fiber reinforced composite model, which is shown in figure36 and 37 respectively. Shear Moduli has increased as the fiber volume percentage increased whereas Poisons ratio was decreased making model more stable. Furthermore, estimation equation was used to verify the Shear Modulus and Poisson's ratio, which is also shown in graph.

Estimation Equations:

$$Gxz = \frac{Ex}{2(1 + \text{vxz})}$$

$$Gxy = \frac{Gxyf \times Gm}{Vf \times Gm + Vm \times Gxyf}$$

$$\text{vzx} = \text{Vf} \times \text{vf} + \text{Vm} \times \text{vm}$$

$$\text{vxz} = \text{vzx} \times \frac{Ex}{Ez}$$

Where,

Gxz = Shear Modulus along plane XZ.

Gxy = Shear Modulus along plane XY.

$vzx = \text{Poissons ratio}$ When load applied to Z direction.

$vxz = \text{Poissons ratio}$ When load applied to X direction.

4.3 VALIDATION

In plane compression test was conducted for the specimens with PLA and CFRPLA materials, which shows that PLA and CFRPLA have similar compressive stress strain pattern. However, PLA specimen have lower Young's Modulus, higher ultimate strength, and better ductility (Plasticity) than the CFRPLA specimen does.

Theoretically, the in-plane stiffness in X and Y directions for the same material and same volume should be equal but due to fiber placement and asymmetric topology Young's Modulus is different. PLA has lower in plane stiffness than CFRPLA in same volume occupied and in same direction because of carbon fiber reinforcement in CFRPLA. The higher the volume occupied by carbon fiber the higher stiffness i.e. Young's Modulus. In modelling of CFRPLA, there is issue of bonding between PLA and carbon fiber and during fabrication of CFRPLA by 3D printing, there is some bonding and internal voids issue this gives more percentage error in modelling and experiment data of CFRPLA than PLA.

During layer-by-layer fabrication of PLA and CFRPLA, the fiber orientation cannot exactly follow the printing path and randomness is not same as modelling, which becomes the factor for error.

The testing and modeling data of Young's modulus considering the fiber orientation in the specimens fabricated by 3D printing is listed. Table 15 and table 16 shows the experimental and modeling Young's Modulus data for PLA and CFPLA respectively.

Table 16: Young's Modulus of PLA by testing and modeling.

Volume	Direction	PLA		
		Experiment (GPA) (Deviation GPA/vol%)	Simulation (GPA) (vol%)	Difference (%)
50% Volume occupied	EX	0.455 (0.0083/52.6%)	0.461 (51.5%)	1.32%
	EY	0.505 (0.0783/51.2%)	0.55 (51.5%)	8.91%
80% Volume occupied	EX	1.291 (0.0455/81%)	1.299 (80.9%)	0.62%
	EY	1.493 (0.0205/80%)	1.436 (80.9%)	3.80%

Table 127: Young's Modulus of CFPLA by testing and modeling.

Volume	Direction	CFPLA		
		Experiment (GPA) (Deviation GPA/vol%)	Simulation (GPA) (vol%)	Difference (%)
50% Volume occupied	EX	0.588 (0.0523/50%)	0.7245 (51.5%)	23.20%
	EY	0.622 (0.0262/50.8%)	0.86 (51.5%)	38.30%
80% Volume occupied	EX	1.6 (0.0688/78.9%)	1.855 (80.9%)	15.90%
	EY	2.046 (0.0014/78.1%)	2.018 (80.9%)	1.37%

5. CONCLUSION

Computer based modeling approach can be used to effectively predict mechanical property of discontinuous fiber reinforced composites. One-step method was used to extract the material property of unidirectional fiber reinforced composite where discontinuous fiber reinforced composite was represented by cuboid model.

Two-step Monte Carlo approach was taken to find material property of 3D model where each element represented an element of composites reinforced with unidirectional randomly oriented fibers. Mechanical property i.e. Young's Modulus, Shear Modulus and Poisson's ratio were predicted by tensile test and shear test on REV.

Cuboid unit cell of discontinuous fiber reinforced composites were taken with different fiber aspect ratio and different volume percentage. The modeling result shows that Young's moduli and shear moduli of a discontinuous fiber reinforced composite along fiber direction were significantly higher than the matrix material. Young's moduli and shear moduli for transverse direction of fiber for all fiber aspect ratio and volume percentage was noticeably higher than matrix material but Poisson's ratio was decreased as the fiber aspect ratio and volume percentage of fiber increased except for one dimensional discontinuous fiber reinforced composite when load was applied on transverse direction and strain was measured on another transvers direction i.e. for our model γxy. For Poission's ratio ($\gamma xy = \gamma yx$) as the fiber aspect ratio was increasing the Poisson's ratio was increasing and again Poisson's ratio was increasing with the fiber volume percentage.

Overall, the model had higher Young's moduli, shear moduli and lower Poisson's ratio making our model more structurally stiff and stable than the matrix material as the fiber aspect ratio and fiber volume percentage goes on increasing.

Furthermore, there is always room for improved model analysis and asymmetric models with specific application can be modeled and analyzed to obtain strain, stress and failures like buckling. Aspect ratio of fiber can be increased above 100 and volume percentage of fiber above 25% in order to predict Young's Modulus and Shear Modulus with higher accuracy.

REFERENCES

1. *Hu, Zhong & Karki, Ranjan. (2015). Prediction of mechanical properties of three-dimensional fabric composites reinforced by transversely isotropic carbon fibers. Journal of Composite Materials. 49. 1513-1524. 10.1177/0021998314535960.*

2. *Crutis, P. T., Bader, M. G. and Bailey, J. E., "The stiffness and strength of a polyamide thermoplastic reinforced with glass and carbon fibers", Journal of Material Science, Vol. 13, 1978, p.377-390.*

3. *Sedyono, Joko & Hadavinia, Homayoun & Deng, Jiamei & Marchant, D & Garcia, J. (2012). Optimization of the stacking-sequence of laminated composite plates under buckling loads.*

4. *Rahmanian, Saeed & Abdul Rashid, Suraya & Aziz, Shazed & Zahari, Rizal & Zainudin, E. S.. (2014). Mechanical characterization of epoxy composite with multiscale reinforcements: Carbon nanotubes and short carbon fibers. Materials and Design. 60. 34-40.10.1016/j.matdes.2014.03.039.*

5. *Hosoi, Atsushi & TERAUCHI, Motoki & TSUNODA, Dai & KIMURA, Tatsuya & KOBIKI, Akira & Kawada, Hiroyuki. (2017). Evaluation of initiation and multiplication of transverse crack in cross-ply CFRTP laminates at elevated temperatures. Transactions of the JSME (in Japanese). . 10.1299/transjsme.17-00312.*

6. *S.-Y. Fu and B. Lauke, Effects of fiber length and fiber orientation distributions on the tensile strength of SFRP. Composites Science and Technology, 1996. 56: p. 12.*

7. *Fu, S.-Y & Lauke, B & Mäder, Edith & Yue, Chee & Hu, Xiao (Matthew. (2000). Tensile properties of short-glass-fiber- and short-carbon-fiber-reinforced polypropylene composites. Composites Part A: Applied Science and Manufacturing. 31. 1117-1125. 10.1016/S1359-835X(00)00068-3.*

8. *M. Hashimoto, T. Okabe, T. Sasayama, H. Matsutani, and M. Nishikawa, Prediction of tensile strength of discontinuous carbon fiber/polypropylene composite with fiber orientation distribution. Composites Part a-Applied Science and Manufacturing, 2012.*

9. *Hu, Zhong & Thiyagarajan, Kaushik Venugopalan & Bhusal, Amrit & Letcher, Todd & Hua Fan, Qi & Liu, Qiang & Salem, David. (2017). Design of ultra-lightweight and high-strength cellular structural composites inspired by biomimetics. Composites Part B Engineering. .10.1016/j.compositesb.2017.03.033*

10. *Thomason, J. L. and Vlug, M. A., "Influence of fiber length and concentration on the properties of glass fiber-reinforced polypropylene: Part 1. Tensile and flexural modulus", Composites Part A, Vol. 27A, 1996, p. 477-484.*

11. *Hahn, H. T., "On Approximations for Strength of Random Fiber Composites", Journal of Composite Materials, Vol. 9, 1975, p. 316-326.*

12. *Thompson, J. L., Vlug, M. A., Schipper, G. and Krikort, H.G.L.T., "Influence of fiber length and concentration on the properties of glass fiber-reinforced polypropylene: Part 3. Strength and strain at failure", Composites Part A, Vol. 27A, 1996, p.1075-1084.*

13. *Manera, M., "Elastic properties of randomly oriented short fiber-glass composites", Journal of Composite Materials, Vol. 11, 1977, p. 235-247.*

14. *Blumentritt, B. F., VU, B. T. and Cooper, S. L., "Mechanical properties of Oriented Discontinuous Fiber Reinforced Thermoplastics. I. Unidirectional Fiber Orientation", Polymer Engineering and Science, Vol. 14, No. 9, 1974, p.633-640.*

15. *Tucker III, C. L., and Liang, E., "Stiffness prediction for unidirectional short-fiber composites: Review and evaluation", Composites Science and Technology, No. 59, 1999, p.655-671.*

16. *Kuriger, R. J. and Alam, M. K., "Strength Prediction of Partially Aligned Discontinuous Fiber-reinforced Composites", Journal of Material Response, Vol. 16, No.1, 2001, p.226-232.*

17. *Mechanical Behavior of Materials –Engineering Methods for Deformation, Fracture, and Fatigue-Norman E. Dowling.*

18. *Global Resources for injection molding. Available from: http://www.injectionmoldingonline.com/Molding101/InjectionMolding.aspx.*

19. *Veen Filament Wound Carbon. Available from: http://www.venn-cycling.com/index.php/rims/filament-wound-rims.*

20. *A Guide to 3D Printing. Available from: https://megadepot.com/resource/a-guide-to-3d-printing.*

21. *Composite Testing For Different Application. Available from: https://www.industrialheating.com/articles/92550-composites-testing-for-aerospace-applications?v=preview.*

22. *Wilk D. Biomimicry: innovation inspired by nature. Cah Du Cine 2002;6:52-5.*

23. *Mittal V, Saini R, Sinha S. Natural fiber-mediated epoxy composites: a review. Compos Part B 2016;99:425-35.*

24. *Morozov, V. V. (2013). Advanced Mechanics of Composite Materials and Structural Elements. Burlington: Elsevier Science*

25. *Cadman, J. (2012). The design of cellular materials inspired by nature-characterization. Design and fabrication. University of Sydney.*

26. *Sherrard KM. Cuttlebone morphology limits habitat depth in eleven species of Sepia (Cephalopoda: sepiidae). Biol Bull-Us 2000;198:404-14.*

27. *Fauziyah S, Soesilohadi RCH, Retnoaji B, Alam P. Dragonfly wing venous crossjoints inspire the design of higher-performance bolted timber truss joints. Compos Part B 2016;87:274-80.*

28. *Mayer G. Rigid biological systems as models for synthetic composites. Sci 2005;310:1144-7*

29. *Barthelat F, Espinosa HD. Elastic properties of nacre aragonite tablets. In: The 2003 SEM annual conference and exposition on experimental and applied mechanics; 2003. Charlotte, North Carolina.*

30. *Kolednik O, Predan J, Fischer FD, Fratzl P. Bioinspired design criteria for damageresistant materials with periodically varying microstructure. Adv Funct Mater 2011;21:3634-41.*

31. *Burns L, Mouritz AP, Pook D, Feih S. Bio-inspired hierarchical design of composite T-joints with improved structural properties. Compos Part B 2015;69:222-31.*

32. *Kolednik O, Predan J, Fischer FD, Fratzl P. Bioinspired design criteria for damageresistant materials with periodically varying microstructure. Adv Funct Mater 2011;21:3634-41.*

33. *Zhou S, Li Q. The relation of constant mean curvature surfaces to multiphase composites with extremal thermal conductivity. J Phys D Appl Phys 2007;40: 6083-93. 82*

34. *Zhou S, Li Q. The relation of constant mean curvature surfaces to multiphase composites with extremal thermal conductivity. J Phys D Appl Phys 2007;40: 6083-93. 82*

35. *Dhand V, Mittal G, Rhee KY, Park S-J, Hui D. A short review on basalt fiber reinforced polymer composites. Compos part B 2015;73:166-80. 83*

36. *Sebastian W, Gegeshidze G, Luke S. Positive and negative moment behaviours of hybrid members comprising cellular GFRP bridge decking epoxy-bonded to reinforced concrete beams. Compos Part B 2013;45(1):486-96.*

37. *Kruijf ND, Zhou S, Li Q, Mai YW. Topological design of structures and composite materials with multiobjectives. Int J Solids Struct 2007;44:7092-109.*

38. *Cheung H-A, Lau K-T, Lu T-P, Hui D. A critical review on polymer-based bioengineered materials for scaffold development. Compos part B 2007;38(3): 291- 300.*

39. *Gower D, Vincent J. The mechanical design of the cuttlebone and its bathymetric implications. Biomimetics 1996;4:37-58.*

40. *Lepore E, Faraldi P, Bongini D, Boarino L, Pugno N. Plasma and thermoforming treatments to tune the bio-inspired wettability of polystyrene. Compos Part B 2012;43(2):681-90.*

41. *Koronis G, Silva A, Fontul M. Green composites: a review of adequate materials for automotive applications. Compos Part B 2013;44(1):120-7.*

42. *Huda S, Reddy N, Yang Y. Ultra-light-weight composites from bamboo strips and polypropylene web with exceptional flexural properties. Compos Part B 2012;43(3):1658-64.*

43. *Okereke MI, Akpoyomare AI, Bingley MS. Virtual testing of advanced composites, cellular materials and biomaterials: a review. Compos Part B 2014;60: 637-62.*

44. *Affatato S, Ruggiero A, Merola M. Advanced biomaterials in hip joint arthroplasty: a review on polymer and ceramics composites as alternative bearings. Compos Part B 2015;83:276-83.*

45. *Dai, Gaoming, and Weihong Zhang. "Size Effects of Effective Young's Modulus for Periodic Cellular Materials." Science in China Series G: Physics, Mechanics and 86 Astronomy Sci. China Ser. G-Phys. Mech. Astron. 52, no. 8 (2009): 1262-270. doi:10.1007/s11433-009-0151-9.*